

EXCHANGE OF NITROGEN AND PHOSPHORUS BETWEEN A SHALLOW ESTUARY
AND COASTAL WATERS

A Thesis

Presented to the Faculty of the Graduate School

of Cornell University

in Partial Fulfillment of the Requirements for the Degree of

Master of Science

by

Melanie Hayn

May 2012

© 2012 Melanie Hayn

ABSTRACT

The nitrogen load to West Falmouth Harbor has increased dramatically over the past decade with no concomitant increase in phosphorus load. In this study, I measured exchange of nitrogen and phosphorus between the harbor and coastal waters over several years. During summer months the harbor retained the entire nitrogen load from the watershed and had an additional net nitrogen input from exchange with coastal waters on many days. During the spring and fall there was a net export of nitrogen from the harbor to coastal waters. Annually, the harbor retained approximately half of the nitrogen load from the watershed. For phosphorus, the harbor had a net import from coastal waters in the spring and summer months and a net export in the fall. Despite the large increase in nitrogen load to the harbor, the summertime import of phosphorus from nearshore waters is sufficient to maintain nitrogen limitation.

BIOGRAPHICAL SKETCH

Melanie was born to Deborah (Webster) and Jeffrey Hayn on January 22, 1982 in Middletown, Connecticut, and grew up with her brother, Colin, in Colchester, Connecticut. She spent many summers with her grandparents on Cape Cod, where she spent long days by the ocean discovering sea creatures and exploring Cape Cod Bay on her grandfather's boat. On one occasion in elementary school after a visit to the research vessels in Woods Hole, she decided that she was going to grow up to be a marine biologist and work in Woods Hole, a surprisingly accurate prediction. She attended public schools in Colchester, and was fortunate to have incredibly engaging teachers and the opportunity to participate in many extracurricular activities. The most influential of these was Project Oceanology, where she participated in six sessions starting in seventh grade studying marine science and conducted the research for her high school senior project on eutrophication and sediment nutrient storage in the Thames River Estuary.

After graduation, Melanie was awarded a Presidential Research Scholarship at Cornell University, which sponsored her undergraduate research project on carbon and sulfur cycling in biologically rich fens under the supervision of Dr. Barbara Bedford. Pursuing her love of marine science, Melanie spent a semester away from Cornell to participate in the Semester in Environmental Science program offered by the Ecosystems Center of the Marine Biological Laboratory in Woods Hole. She graduated summa cum laude with distinction in research in 2004 with a B.S. in Science of Earth Systems and a concentration in Biogeochemistry, and decided that she wanted to take her research career back to the ocean where it had started.

After graduation, Melanie took a position working for Drs. Robert Howarth and Roxanne Marino at Cornell University, working on a project based out of the Marine Biological Laboratory. This allowed her the opportunity to keep her connection with the Cornell community while living and working in the Woods Hole scientific community, where she has had the opportunity to work with inspiring and enthusiastic colleagues. Her work allows her to study a complex and evolving system which combines her love of chemistry and environmental science with some of her favorite activities, like scuba diving and kayaking. While watching many of her colleagues leave the MBL to pursue graduate degrees, she counts herself fortunate to have been able to continue working on the same research project while simultaneously pursuing her degree, giving her a depth of knowledge that's hard to find in a short term project. She currently lives in Pocasset, MA with her husband, Eli Perrone, where she spends her free time exploring local scuba diving and kayaking spots and playing oboe in several community musical ensembles.

ACKNOWLEDGMENTS

I have been fortunate during the completion of this research to work with a large group of colleagues from several institutions who have generously shared their expertise, time, and talent. Over the seven years I have been involved with the West Falmouth Harbor project, I have gained insight from my many colleagues from Cornell, the Marine Biological Laboratory (MBL), University of Virginia, US Geological Survey, and CR Environmental, Inc. This work was made possible with funding from a NSF Biocomplexity Coupled Biogeochemical Cycles Grant, as well as from the Woods Hole Seagrant Foundation and the NSF Biogeochemistry and Environmental Biocomplexity program at Cornell.

I cannot extend enough thanks to my committee chair and supervisor, Bob Howarth, for his support, encouragement, and flexibility as I navigated this journey into biogeochemical research. The example he set through his vision and rapid ability to synthesize results into the bigger ecosystems picture was inspiring. I also want to especially thank my immediate supervisor Roxanne Marino. As a fellow detail-oriented individual, I have benefited from her advice in all areas from laboratory and field procedures to balancing my work and personal life. In a complicated situation involving off-campus research and pursuing an employee degree, their support and confidence has allowed me to grow and mature as a researcher. Also, thanks to Pat Sullivan for being a member of my committee; his willingness to meet with me to discuss new ways to look at my data, assist with statistical analyses, and provide objective feedback on my writing was invaluable.

In 2005, I began my work on this project as part of a large team of principal investigators, research assistants, and students to whom I owe deep thanks for all their help and support. Sam Kelsey has always been available for logistical assistance with laboratory and field work and has practical advice for just about any situation. Jane Tucker has always shared her wealth of practical knowledge and experience with me, and without Clara Funk's optimism and enthusiasm for all tasks in the lab and field I'm not sure I would have made it through some of our sampling expeditions with my sanity intact. I also want to thank the other principal investigators on the project, Anne Giblin, Ken Foreman, Karen McGlathery, and Peter Berg, for sharing their wisdom and vision with me over the years. Anne and Sam also deserve credit for educating me in the ways of expertly collecting delicate samples while diving in water with the consistency of pea soup. I also want to thank the other research assistants and students who provided assistance and companionship during my studies, including Neil Bettez, Laura Wittman, Ursula Mahl, Natalie McLenaghan, Steve Romaniello, Jeff Walker, Meredith Ferdie-Muth, Laura Reynolds, Laura Erban, and Kim Holzer.

My lab mates in the Howarth Lab Group have provided insight and encouragement during my visits to Ithaca; Dennis Swaney, Tom Butler, Bongghi Hong, Marina Molodovskaya, and Renee Santoro. Despite my unpredictable schedule, they were always willing to make time for me during my visits and provide a morale boost during stressful times. Particular thanks to Dennis Swaney for his patient advice and perspective on modeling, math, and wine. As an off-campus employee, I am also fortunate to have had the support of the dedicated administrative staff both at Cornell and the MBL to deal with a number of unique logistical tasks. Thanks to LuAnne Kenjerska and DeeDee Albertsman, who helped me navigate the tricky financial waters

of off-campus purchases, particularly during the acquisition of reliable field transportation (our boat). My appreciation also goes to Kelly Holzworth, for her advice and assistance in all aspects of the logistics involved with being a visitor to the MBL, and to the Ecosystems Center for providing both office and research space.

I also would like to acknowledge our colleagues at the US Geological Survey, who we collaborated with on our hydrological work; Chris Sherwood and Neil Ganju. Their enthusiasm and implementation of state of the art sampling techniques were inspiring. The folks at CR Environmental were also incredibly supportive, including Chip Ryther, Charlotte Cogswell, and Eli Perrone, and their willingness to loan me survey equipment and expertise was instrumental in my success in this project.

Family has been the foundation of all that I've accomplished in my life. I owe my family a debt of gratitude for all the love and support they've offered through my graduate work, as well as for all the logistical and emotional support in the years leading up to my involvement in this project. Without their willingness to help me pursue my interests I wouldn't be here now. I owe the biggest thanks to my husband, Eli Perrone, for all those weekends we spent out in a skiff with survey equipment or hiking the perimeter of the harbor with a backpack full of gear, for the days spent deploying and re-engineering field gear or in the garage bottom-painting the boat or disassembling the outboard, and for reading all those drafts and commenting on countless preliminary PowerPoint presentations; I never could have done this without your skill and support.

TABLE OF CONTENTS

| | |
|--|-----|
| BIOGRAPHICAL SKETCH | iii |
| ACKNOWLEDGMENTS | v |
| LIST OF FIGURES | x |
| LIST OF TABLES | xii |
| EXCHANGE OF NITROGEN AND PHOSPHORUS BETWEEN A SHALLOW ESTUARY AND COASTAL WATERS | 1 |
| Abstract | 1 |
| Introduction | 2 |
| Methods | 5 |
| <i>Study Site</i> | 5 |
| <i>Nitrogen load calculation</i> | 6 |
| <i>Water Exchange</i> | 9 |
| <i>Nutrient Concentrations</i> | 11 |
| <i>Nutrient Exchange Calculation</i> | 14 |
| Results and Discussion | 16 |
| <i>Nitrogen Load</i> | 16 |
| <i>Harbor Physical Parameters and Bathymetry</i> | 19 |
| <i>Water Exchange</i> | 21 |
| <i>Nutrient Concentrations</i> | 22 |
| <i>Nutrient Mass Exchange Fluxes</i> | 28 |
| <i>Seasonal Nutrient Exchange and Retention</i> | 30 |
| <i>Annual Nitrogen Exchange and Retention</i> | 34 |
| Conclusion | 37 |
| APPENDIX 1: Spatial Modeling in Estuaries: Using Ordinary Kriging to Estimate Tidal Water Flux in West Falmouth Harbor | 38 |
| Methods | 39 |

| | |
|---|----|
| <i>Bathymetric data collection</i> | 39 |
| <i>Spatial Interpolation</i> | 40 |
| <i>Volume Estimation</i> | 42 |
| <i>Water Flux Calculation – Volumetric Change Method</i> | 43 |
| <i>Water Flux Calculation – Index Velocity Method</i> | 45 |
| Results | 45 |
| <i>Model Fit and Predictions – Bathymetry Interpolation</i> | 45 |
| <i>Volume and Standard Error</i> | 49 |
| <i>Continuous Tidal Water Fluxes</i> | 51 |
| Discussion | 53 |
| APPENDIX 2: Estimation of the Importance of Ammonia Volatilization in Nitrogen Flux Estimates in West Falmouth Harbor | 55 |
| APPENDIX 3: Using Side Scan Sonar for Seagrass Distribution in West Falmouth Harbor | 61 |
| Methods | 61 |
| Results and Discussion | 63 |
| REFERENCES | 67 |

LIST OF FIGURES

| | |
|--|----|
| Figure 1. Map of West Falmouth Harbor highlighting the sites most impacted by enriched groundwater (Snug Harbor and Mashapaquit Creek), as well as the less impacted Outer Harbor. | 6 |
| Figure 2. Watershed delineations from Howes <i>et al.</i> (2006) overlain on the land use classifications provided by the Town of Falmouth. | 8 |
| Figure 3. Nitrate concentrations as a function of salinity in Snug Harbor and Mashapaquit Creek during low-tide sampling in the winters of 2011 and 2012. The zero-salinity intercepts represent the average nitrate concentration in fresh water entering these basins. | 17 |
| Figure 4. Variations in water level elevation over a one month timeframe in 2007. Water levels are relative to a benchmark set up on the West Falmouth Town dock. | 19 |
| Figure 5. Bathymetric map of West Falmouth Harbor based on surveys conducted during the summer of 2008. Depths are in meters below mean higher high water. | 20 |
| Figure 6. Comparison of a one-month sampling period in August and September 2010 calculated using index velocity and volumetric change methods. | 21 |
| Figure 7. Histograms of observed concentrations of dissolved and total N and P over the entire observation period, encompassing spring, summer, and fall samples. | 23 |
| Figure 8. Boxplots showing the median, middle 50%, and full range of observations of N and P by season alongside the mean and 95% confidence interval on the mean. | 24 |
| Figure 9. Patterns of nutrient concentration on September 25, 2006. Both DIN and TN were higher when the tide was flowing out than when the tide was coming in, while there is no apparent difference in either SRP and TP between flood and ebb tides. | 25 |
| Figure 10. Patterns of nutrient concentration on May 31, 2006. On this date, there were statistically higher concentrations of DIN, TP, SRP, and TP when the tide was flowing out compared to when the tide was coming in. | 26 |
| Figure 11. Patterns of nutrient concentration on July 8, 2008. In contrast to the previous two figures, there was no statistically significant difference in either DIN or TN between flood and ebb tide. | 27 |
| Figure 12. Daily estimates of net TN exchange calculated with the 95% confidence interval. | 29 |
| Figure 13. Daily estimates of net TP exchange with the 95% confidence interval indicated. | 30 |

| | |
|---|----|
| Figure 14. Seasonally averaged fluxes of DIN, TN, SRP, and TP. Generally, we see a net import of DIN, TN, SRP, and TP during the summer, a net export in the spring, and a net export of N but net import of P in the fall. | 31 |
| Figure 15. Relationship between N retention and the ratio of depth to residence time for North American and European estuaries. | 36 |
| Figure A1–1. Map of bathymetric data used as model input. | 40 |
| Figure A1–2. Locations of validation points are shown in blue. Gray points are the original observations used to create the interpolation model. | 42 |
| Figure A1–3. Exponential semivariogram fit by weighted least squares in S-Plus | 46 |
| Figure A1–4. Kriged surface of the estuary at a regular grid of prediction locations. | 47 |
| Figure A1–5. Standard error surface resulting from kriging analysis. | 48 |
| Figure A1–6. Predicted values of harbor depth from the kriged model compared to the observed depth values for the validation data transect. | 48 |
| Figure A1–7. Residuals for the validation dataset. | 49 |
| Figure A1–8. Relationship between water level and volume of the harbor, with prediction line from polynomial linear model fit, second order. | 50 |
| Figure A1–9. Comparison of water fluxes using the index velocity method and volumetric change method during a full tidal cycle during a spring tide on August 9, 2010. | 51 |
| Figure A1–10. Comparison of a one-month sampling period in August and September 2010 over a full spring-neap cycle of water fluxes calculated using index velocity and volumetric change methods. | 52 |
| Figure A1–11. Residuals of the flow rate comparison between the index-velocity method and the volumetric change method on 8/9/10. | 52 |
| Figure A2–1. Change in ammonia volatilization rates as dissolved ammonium concentrations within the harbor increase above present levels (present average: 0.3 μ M). | 60 |
| Figure A3–1. Side scan sonar image example, showing the edge of the seagrass bed and bare patch around a mooring. | 62 |
| Figure A3–2. The seagrass extent resulting from side scan analysis for 2010. | 64 |
| Figure A3–3. The difference in seagrass extent over time as mapped by the Department of Environmental Protection in 1995, 2001, and 2006 in comparison with my 2010 seagrass extent mapped from side scan sonar imagery. | 66 |

LIST OF TABLES

| | |
|---|----|
| Table 1. Start dates for nutrient sampling deployments arranged by season | 12 |
| Table 2. Detection limits for nutrient analyses | 14 |
| Table 3. Physical parameters of West Falmouth Harbor based on bathymetry and water level elevation | 20 |
| Table A1–1. Comparison of volume, SSE, and SE as a percent of the predicted volume at different water levels | 50 |
| Table A2–1. Summary of ammonia volatilization rates for individual summertime days sampled, as well as the rate calculated by combining data from individual sites on days with maximum volatilization rates. | 59 |
| Table A3–1. Comparison of seagrass areas estimated from side scan sonar surveys (this study; 2010) with previous areal estimates from surveys conducted by the MA DEP (1995, 2001, 2006). | 65 |

EXCHANGE OF NITROGEN AND PHOSPHORUS BETWEEN A SHALLOW ESTUARY AND COASTAL WATERS

ABSTRACT

The nitrogen load to West Falmouth Harbor increased dramatically over the past decade with no concomitant increase in phosphorus load due to input of nitrogen-contaminated groundwater from a wastewater treatment facility. I estimate that by 2010 this input of contaminated groundwater had increased the total nitrogen load by 3-fold compared with background loading. In this study, I measured exchange of nitrogen and phosphorus between the harbor and coastal waters on 24 days during spring, summer, and fall over several years. The patterns of exchange were similar for both inorganic and organic nutrients, but the net exchanges of organic nitrogen and phosphorus were generally greater than for inorganic forms in the spring and summer months. Nutrient exchanges varied seasonally. During summer months, the harbor retained the entire nitrogen load from the watershed and had an additional net nitrogen input from the exchange with coastal waters on many days. During the spring and fall, there was a net export of nitrogen from the harbor to coastal waters. Annually, the harbor retained approximately half of the nitrogen load from the watershed, in reasonable agreement with predictive relationships for nitrogen retention as a function of the ratio of depth to water residence time developed in other estuaries, most of which were deeper and had longer water residence times. For phosphorus, the harbor had a net import from coastal waters in the spring and summer months and a net export in the fall months. Despite the large increase in nitrogen

load to the harbor, the summertime import of phosphorus from nearshore waters is sufficient to maintain nitrogen-limiting conditions for primary producers in the system.

INTRODUCTION

Nutrient fluxes to the coastal zone have been increasing over the past several decades as a result of human activities, leading to increased loading to coastal estuaries and embayments (NRC 2000; Rabalais 2002; Billen *et al.* 2011; Howarth *et al.* 2011). As of the beginning of the century, approximately two thirds of the estuaries in the United States were moderately to severely degraded from nutrient pollution (Bricker *et al.* 1999, 2007; NRC 2000).

Shallow estuaries are particularly sensitive to nutrient pollution (Valiela *et al.* 1997; NRC 2000, Nixon *et al.* 2001). They also have a more complicated response to nutrient enrichment than deeper systems, and as a result this response is not as well understood (Nixon *et al.* 2001; McGlathery *et al.* 2007; Howarth *et al.* 2011). In shallow systems, light penetrates to the sediment which results in primary production dominated by benthic plants, algae, and cyanobacteria rather than phytoplankton (Valiela *et al.* 1997; McGlathery *et al.* 2001, 2008). Since these benthic primary producers (particularly seagrasses) can accumulate a large standing stock of biomass during the growing season, seasonal retention of nutrients can be high compared to phytoplankton-dominated systems (Duarte and Cebrian 1996; Nixon *et al.* 2001) and nutrient concentrations in the water column tend to be lower (Nixon *et al.* 2001; McGlathery *et al.* 2007).

Nitrogen (N) loading in particular has been shown to be the primary driver of eutrophication in many coastal ecosystems (i.e. Vitousek and Howarth 1991; Nixon 1995; Blomqvist et al 2004; Howarth and Marino 2006; Conley *et al.* 2009). One potential mechanism for maintaining N limitation despite large terrestrial N inputs is exchange with coastal waters that often have relatively high phosphorus (P) concentrations and low N:P ratios as a result of denitrification on the continental shelf (Howarth *et al.* 2011). A large input of N compared to P from exchange with coastal waters has been observed in Chesapeake Bay (Boynton *et al.* 1995) and the Yangtze River (Li *et al.* 2011).

The retention of terrestrial N load in coastal systems has been examined in several North American and European estuaries on an annual timescale, and reviews of data from these systems show a relationship between percent N retention and the ratio of average water depth to residence time (Nixon *et al.* 1996; Billen *et al.* 2011). The estuaries in these studies were predominately deeper, plankton-dominated systems, and N retention was ascribed largely to denitrification, which is greater in ecosystems with longer residence times and comparatively shallower depths due to greater water contact time with the sediment (Nixon *et al.* 1996). Nitrogen retention has been little studied in shallow estuaries where benthic primary producers are dominant. Assimilation of N by these benthic primary producers would be expected to also contribute significantly to N retention, at least on a seasonal basis (McGlathery et al. 2007).

Despite the large body of research on the effects of N enrichment over the past half century, there have been few whole-ecosystem studies of the impacts of increased N supply to either deep estuaries or shallow coastal bays, and none to my knowledge where there was not

an accompanying increase in P load. Studies of this nature are essential to understanding the complicated biogeochemical feedbacks in coastal systems.

West Falmouth Harbor is a small coastal lagoon that has been experiencing rapid degradation as a result of a plume of N-rich groundwater which began entering the harbor in the late 1990's and increased greatly in the mid 2000's (Howes *et al.* 2006). The plume originates at the Falmouth Wastewater Treatment Facility, which is located 1km away from the easternmost part of the harbor and discharged secondarily treated wastewater into the groundwater on site from 1986-2005 through infiltration, spray irrigation, and ground injection (Jordan *et al.* 1997; Sterns and Wheler 2001; Howes *et al.* 2006; Town of Falmouth 2011). This groundwater takes many years to travel from the treatment plant to the harbor, estimated at 7-10 years (Kroeger *et al.* 2006), and during this travel through the soil nearly all of the P is removed from the effluent as a result of sorption to aquifer minerals (Weiskel and Howes 1992). Previously, development within the watershed had only led to mild impairment of water quality in the estuary, but by 2005 the harbor exhibited areas with moderate to severe habitat degradation as a result of this large increase in N load (Howes *et al.* 2006).

West Falmouth Harbor provides an ideal location to study the effects of N enrichment as a result of the dramatic increase in N load with no change in the P load. Although several studies have looked at the watershed loading to the harbor (Hamilton 1995; Kroeger 2006; Howes *et al.* 2006), none have done so in the past several years, when we expect the peak N loading rate. Also, nutrient exchange between the harbor and the coastal waters of Buzzards Bay has not been measured previously. The main purpose of this study is to quantify the exchange of N and P between West Falmouth Harbor and the coastal waters of Buzzards Bay.

Additionally, I quantify the N load from the contaminated groundwater plume to examine the ability of the harbor to retain this large increase in N load.

METHODS

Study Site

West Falmouth Harbor is a small, approximately 70 ha, shallow lagoon located in the town of Falmouth, MA (41.36°N, 70.38°W). The harbor exchanges water with the adjacent coastal waters of Buzzards Bay through a well-constrained inlet 3m deep and 150m wide. The harbor can be divided into sub-basins based on flushing time and geography (Figure 1). Of particular importance when considering the nutrient dynamics of this system are the Outer Harbor, the portion near the mouth that exchanges rapidly with Buzzards Bay, and Snug Harbor, the northeast corner of the inner harbor where most of the enriched groundwater is entering. A small groundwater-fed creek called Mashapaquit Creek feeds directly into Snug Harbor from the northeast, and is considered a basin of the estuary in my analysis since it exchanges water tidally with Snug Harbor. The estuary is tidally dominated, with all freshwater inputs coming from precipitation and groundwater. In comparison with tidal exchange, the groundwater inputs to the estuary are quite small, estimated at $18,000 \text{ m}^3 \text{ d}^{-1}$ (Ganju *et al.* 2012). Approximately half of the groundwater inputs to the harbor enter in the northeast region of the harbor in the Mashapaquit Creek and Snug Harbor areas (Howes *et al.* 2006, Kroeger *et al.* 2006). Mean system residence time in Snug Harbor is five days (Howes *et al.* 2006), somewhat longer than for the harbor as a whole where the system residence time is approximately one day (Howes *et al.* 2005, Ganju *et al.* 2012).

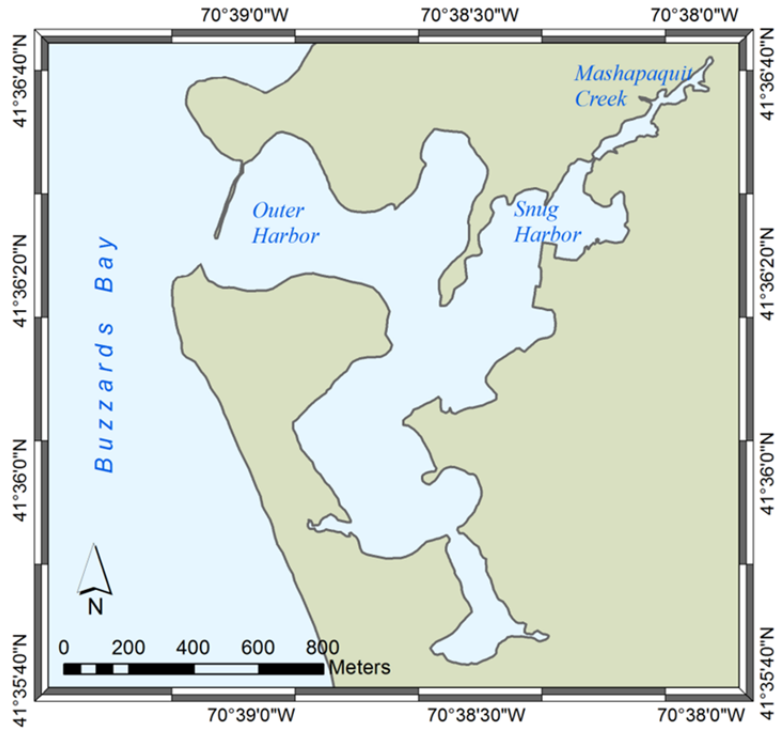


Figure 1. Map of West Falmouth Harbor highlighting the sites most impacted by enriched groundwater (Snug Harbor and Mashapaquit Creek), as well as the less impacted Outer Harbor.

Nitrogen load calculation

I calculated the average N load to West Falmouth Harbor between 2005 and 2009 by dividing the load into three components, the elevated load from the contaminated groundwater plume, the background load coming from all other sources in the watershed (both anthropogenic and natural), and a term for the direct atmospheric deposition of N onto the water surface of the harbor. This can be represented by the following equation,

$$N Load_{total} = N Load_{back} + N Load_{plume} + N Load_{dep} \tag{1}$$

where $N\text{ Load}_{\text{total}}$ is the total load to the harbor, $N\text{ Load}_{\text{back}}$ is background load from the watershed, $N\text{ Load}_{\text{plume}}$ is the load from the contaminated groundwater plume, and $N\text{ Load}_{\text{dep}}$ is the nitrogen load from direct atmospheric deposition onto the water surface, all in kmol N d^{-1} .

Kroeger *et al.* (2006) estimated the total background load ($N\text{ Load}_{\text{back}}$) as 0.8 kmol N d^{-1} . I derived a separate estimate from Howes *et al.* (2006) by subtracting their estimate for the contaminated plume from their estimate of total watershed load. This results in 1.0 kmol N d^{-1} . I used the average of these two estimates for the background load from the watershed, or 0.9 kmol N d^{-1} . Since land use in the watershed has not changed significantly over the past decade, these estimates are still an appropriate representation of the background load to the harbor. I estimated the direct atmospheric N load to the water surface ($N\text{ Load}_{\text{dep}}$) as 0.2 kmol N d^{-1} , by applying the average deposition rate of $15\text{ kg N ha}^{-1}\text{ yr}^{-1}$ on Cape Cod from Bowen and Valiela (2001) to the mean harbor surface area.

To quantify the loading from the contaminated groundwater plume in excess of the background loading, I separately evaluated the two sub-basins that receive water from the plume, Snug Harbor and Mashapaquit Creek, based on the watershed delineations from Howes *et al.* (2006) shown in Figure 2.

$$N\text{ Load}_{\text{plume:MC}} = (10^{-6} * Q_{MC} * C_{MC}) - B_{NO3:MC} \quad (2)$$

$$N\text{ Load}_{\text{plume:SH}} = (10^{-6} * Q_{SH} * C_{SH}) - B_{NO3:SH} \quad (3)$$

where $N\text{ Load}_{\text{plume:MC}}$ and $N\text{ Load}_{\text{plume:SH}}$ are the nitrate loads in the groundwater plume from the treatment plant that enter Mashapaquit Creek and Snug Harbor, respectively (kmol d^{-1}). Q_{MC} and Q_{SH} are the mean groundwater flow rates into Mashapaquit Creek and Snug Harbor in m^3

d^{-1} , C_{MC} and C_{SH} are the average concentrations of nitrate in groundwater flowing into Mashapaquit Creek and Snug Harbor in μM , and $B_{NO_3:MC}$ and $B_{NO_3:SH}$ are the portion of the background load to Mashapaquit Creek and Snug Harbor attributable to nitrate using estimates from Kroeger *et al.* (2006), in $kmol N d^{-1}$.

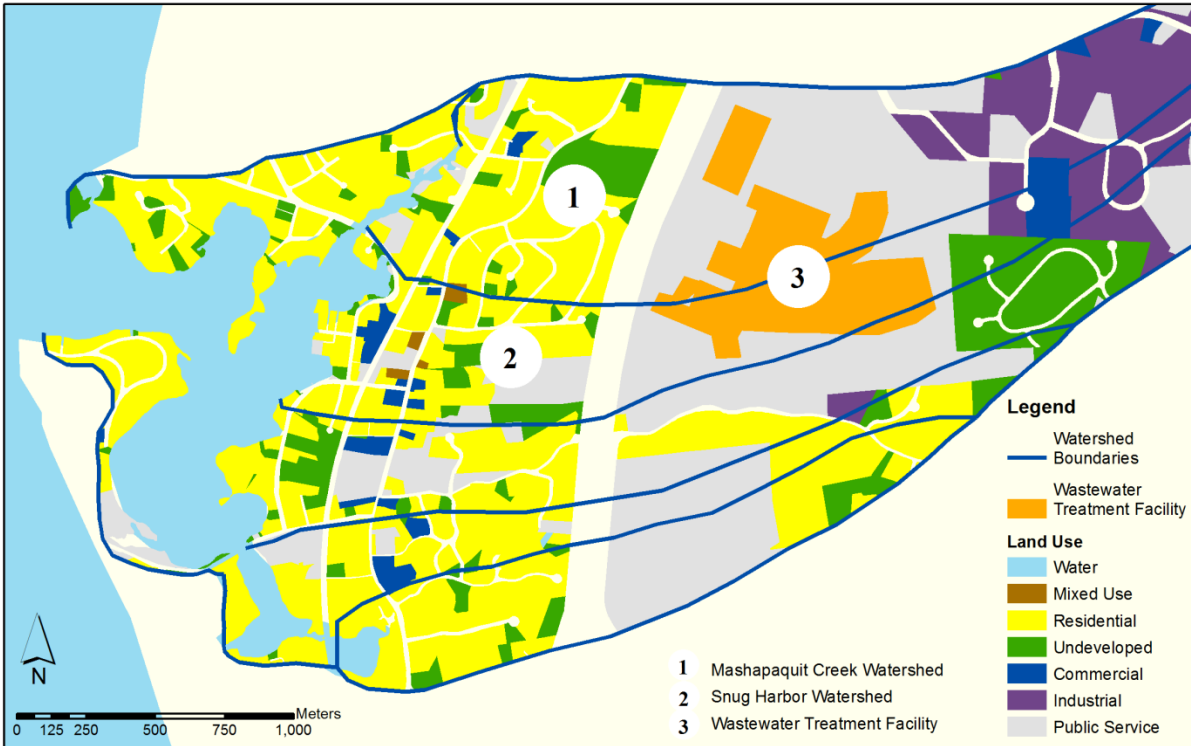


Figure 2. Watershed delineations from Howes *et al.* (2006) overlain on the land use classifications provided by the Town of Falmouth (Office of Geographic Information (MassGIS), Commonwealth of Massachusetts, Information Technology Division). The orange polygon represents the wastewater treatment facility, including the historic spray irrigation area. Note that the treatment facility is almost entirely inside the Snug Harbor and Mashapaquit Creek watersheds, and contaminated groundwater from the facility would be expected to flow down gradient into these areas of the harbor.

For groundwater flow into Mashapaquit Creek (Q_{MC}), I used the estimate of Ganju (2011) based on acoustic measurements: $1,700 m^3 d^{-1}$. For groundwater flow into Snug Harbor (Q_{SH}), I used an estimate for total freshwater input to West Falmouth Harbor from Ganju *et al.*

(2012), $18,100 \text{ m}^3 \text{ d}^{-1}$, apportioned by the result of Kroeger *et al.* (2006) that 35% of all freshwater inputs to West Falmouth Harbor enter through Snug Harbor. I therefore calculate the groundwater flow rate into Snug Harbor (Q_{SH}) as $6,350 \text{ m}^3 \text{ d}^{-1}$.

The nitrate concentration of the contaminated groundwater entering Snug Harbor and Mashapaquit Creek was estimated by simultaneously measuring nitrate and salinity in these receiving waters and using a mixing model to extrapolate to the zero-salinity intercept. This approach works in West Falmouth Harbor because nitrate concentrations are high (above $100 \mu\text{M}$) in the groundwater and very low (below $1 \mu\text{M}$) in the salt water from Buzzards Bay. Data were collected during the winters of 2011 and 2012 during the time period before and just following low tide, when biological activity should have been low and there would have been the smallest dilution of groundwater by water from Buzzards Bay. In 2011, data were collected with an ISUS optical nitrate sensor by colleagues at the US Geological Survey, and the calibration was verified using standard colorimetric methods. In 2012 I collected discrete samples and analyzed them using standard colorimetric methods as described in detail below (*Nutrient Concentrations*). Based on discharge records from the treatment facility, the load to the harbor is expected to have been constant from the mid-2000's through the present (Howes *et al.* 2006), so load calculations made in 2011-2012 are taken as representative of the study period.

Water Exchange

I calculate water exchange between West Falmouth Harbor and Buzzards Bay using a volumetric change model and water budget for the harbor. As described above, inputs to the

harbor come from precipitation and groundwater, and exports via evaporation and net tidal exchange. The core of the volumetric change model is the change in harbor volume over time, modeled as:

$$\frac{dV}{dt} = Q_v + P + G - E \quad (4)$$

where dV/dt is the rate of volume change, Q_v is the water exchange at the mouth, G is groundwater flux, P is precipitation, and E is evaporation (all in $\text{m}^3 \text{s}^{-1}$). Positive values of Q_v indicate inflowing tide. Since Q is several orders of magnitude greater than P , G , and E at any given time, for instantaneous fluxes this model reduces to:

$$\frac{dV}{dt} = Q_v \quad (5)$$

Since we can model the harbor as a standing wave with minimal lag between embayments (Howes *et al.* 2006; Ganju *et al.* 2012), I calculate the volume of water within the harbor at any given time from detailed bathymetry and water level measurements made at one location, and use this to calculate water flux rates.

To determine bathymetry, I collected depth soundings with the assistance of CR Environmental, Inc. We used a Trimble AgGPS Model 132 DGPS with sub-meter accuracy to collect horizontal coordinates, and an ODEC Bathy500MF precision survey fathometer to provide depth soundings at a rate of 5-10 Hz. Data were collected on a regular grid with extra resolution in the intertidal zone, and cross-tie data were gathered for quality control analysis. I processed the sounding data using ArcGIS 9.2 and the Geostatistical Analyst Extension to generate a bathymetric grid with 5m horizontal resolution. Further details on field methods, statistical methods used to generate the bathymetric map, and quality control procedures can

be found in Appendix 1. From the digital bathymetry file in ArcGIS, I calculated the volume of water in the harbor at water levels between lowest low tide and highest high tide and fit a regression to the data ($P < 0.00001$; Appendix 1). I collected water level measurements at five minute intervals using a Global Water WL16 vented, pressure and temperature compensated water level logger (accurate to 0.009m), and used these in the regression to calculate volume.

Water levels in the harbor were recorded continuously during our study period, and I calculated rates of volume change in the harbor (dV/dt) for our nutrient fluxes based on harbor volume (V) over short time intervals ($t_2 - t_1$) using the following equation:

$$\frac{dV}{dt} = \frac{V_2 - V_1}{t_2 - t_1} \quad (6)$$

Nutrient Concentrations

I collected water samples for nutrient analysis at the mouth of the harbor using a Teledyne ISCO 6712 portable sampler. Samples were collected hourly over 23-hour periods on 24 days between July 2005 and August 2009 (Table 1). Samples were taken throughout the year with the highest sampling intensity during the summer season when productivity is highest and the response to nutrient enrichment is of greatest interest. Sample water was stored on ice over the sampling period, and then brought back to the lab. For each hourly sample, I transferred one subsample to an acid-washed HDPE bottle and froze it for later analysis of total N (TN) and total P (TP). I filtered two additional sets of sub-samples through a 0.45 μ m Supor membrane filter and either stored them frozen for silica and nitrate analysis or ran them immediately for ammonium and soluble reactive P (SRP).

| Table 1. Start dates for nutrient sampling deployments arranged by season. | | |
|--|--------------|------------|
| Spring Dates | Summer Dates | Fall Dates |
| 5/31/2006 | 7/28/2005 | 9/28/2005 |
| 6/15/2006 | 8/22/2005 | 10/31/2005 |
| 4/4/2007 | 7/26/2006 | 9/13/2006 |
| 4/24/2007 | 8/8/2006 | 9/26/2006 |
| 5/21/2007 | 8/24/2006 | 10/11/2006 |
| 6/11/2008 | 6/26/2007 | 10/24/2006 |
| | 8/21/2007 | 11/7/2006 |
| | 7/8/2008 | 11/30/2006 |
| | 8/18/2009 | |
| | 8/19/2009 | |

Periodic samplings were also conducted to examine depth profiles of nutrients and to look for stratification effects. For these samplings, surface (0.25m) and bottom (1-1.5m) waters in the Outer Harbor were analyzed on eleven dates between April and September during 2005-2006 to assess stratification near the mouth of the system. They were analyzed for inorganic nutrients using the same methods as the hourly samples as well as for temperature and salinity using a Hydrolab Datasonde 4a.

I analyzed TN and TP samples using a dual digestion method for simultaneous oxidation of nitrogen and phosphorus by persulfate reagent based on the methodology of Koroleff (1983), adjusted to provide optimum recovery in estuarine systems following Marino (2001). Total nutrient analyses were run on unfiltered sample water, so concentration measurements include inorganic forms as well as both dissolved and particulate organic forms. Samples were

analyzed for SRP and digested TP using the standard phosphomolybdate colorimetric reaction (Koroleff 1983).

I analyzed samples for ammonium using the phenolhypochlorite standard colorimetric reaction (Solorzano 1969) read on a Cary Spectrophotometer. Nitrate was analyzed using a modification of the Astoria Pacific standard methodology for cadmium reduction in saline samples (A177), with an artificial seawater carrier matched to the salinity of the samples and an increased sample time to increase accuracy at concentrations below $1\mu\text{M}$, an imidazole buffer to prolong cadmium column life, and a decreased buffer:sample ratio to improve the detection limit. I analyzed TN as nitrate in digested samples using a modification of the method described above for saline samples, with a distilled water carrier to reduce salt load through the column. Since concentrations of TN were not below $1\mu\text{M}$, matrix matching the carrier to the salinity of the samples was not necessary. Dissolved inorganic N (DIN) was calculated as the sum of the ammonium and nitrate concentrations.

I calculated detection limits and confidence intervals for each of the nutrient methods using the methodology of the International Union of Pure and Applied Chemistry (Currie, 1999). Detection limits are defined as the minimum concentration that is statistically distinguishable from the blank with 95% confidence. The values for our analyses are shown in table 2.

| Table 2. Detection limits for nutrient analyses. | |
|--|-----------------|
| Analysis | Detection Limit |
| Ammonium | 0.1μM |
| Nitrate | 0.1μM |
| Total Nitrogen | 1.5μM |
| Phosphate | 0.1μM |
| Total Phosphorus | 0.3μM |

Nutrient Exchange Calculation

To calculate the nutrient exchange between West Falmouth Harbor and Buzzards Bay, I take the general approach summarized in the following equation:

$$Ex = \int_t C * Q \quad (7)$$

where exchange (Ex) over some period of time is equal to the integral of the product of concentration (C) and the water flux (Q) over that time period. In this study, I collected samples hourly over 23-hour periods on 24 separate days and modeled nutrient exchange over individual tidal cycles within each day to obtain rates of nutrient exchange for steady-state conditions with respect to total harbor water volume.

Over short timescales, as shown in equation 5, Q_v (the water flux at the harbor mouth) can be assumed to be equal to the volume change in the harbor over time. This is useful for comparing different measurement methods over time scales on the order of minutes. However, on a tidal timescale the net water exchange between the harbor and bay is closer in magnitude to the evaporation and groundwater input over the same time period (on days with no

precipitation), since tidal flow is bi-directional but groundwater flow and evaporation are uni-directional. As a result, exchange over a tidal cycle is calculated using water flux (Q) from equation 4, applying correction factors for the freshwater flux associated with groundwater ($0.21 \text{ m}^3 \text{ s}^{-1}$; Ganju *et al.* 2012) and evaporation ($0.05 \text{ m}^3 \text{ s}^{-1}$; Ganju *et al.* 2012). Net nutrient exchange can thus be represented as

$$Ex_{tide} = \sum_{i=1}^n \left[\left(\frac{dV_i}{dt} - G + E \right) * C_i * \Delta t \right] \quad (8)$$

where Ex_{tide} is the exchange of a nutrient over a tidal cycle (mol), dV_i/dt , and C_i are the volumetric change rate ($\text{m}^3 \text{ s}^{-1}$) and nutrient concentration (mol L^{-1}) at time step i , Δt is the length of the time step for the instantaneous rate calculation in seconds, G and E are the rate of groundwater inflow and evaporation ($\text{m}^3 \text{ s}^{-1}$), and n is the number of time steps within the tidal cycle. The below equation, a simple rearrangement of equation 8, is the form used to compute the exchanges in S-plus to minimize computational error.

$$Ex_{tide} = \sum_{i=1}^n \left(\frac{dV_i}{dt} * C_i * \Delta t \right) - (G - E) \sum_{i=1}^n (C_i * \Delta t) \quad (9)$$

Since the water levels used to calculate dV/dt were collected at a five minute interval and the nutrient fluxes hourly, I extrapolated both using linear extrapolation between sample points to obtain a continuous dataset. I then used equation 9 to calculate the nutrient exchange (Ex_{tide}) over individual tidal cycles within each sampling day on a 30-minute moving window for start time. The number of tidal cycles evaluated on a given day ranged from 6 to 25,

determined by the daily tidal amplitude and differences between the elevations of consecutive high and low tides within the sample day.

To determine whether there were biases in the rate calculation from the number of daylight hours with a tidal cycle, I examined the individual tidal cycle calculations within each day prior to averaging. I found no significant correlation between number of daylight hours in a tidal cycle and the calculated nutrient flux, so have used a straight average of nutrient exchange for all tidal cycle calculations for each sampling day with error bars representing the 95% confidence interval of the estimates.

RESULTS AND DISCUSSION

Nitrogen Load

In Figure 3, I plot winter nitrate concentrations in Snug Harbor and Mashapaquit Creek as a function of salinity. These mixing curves demonstrate a linear relationship between nitrate and salinity in both of these water basins ($P < 0.00001$), consistent with a lack of biological activity at this time of year. The zero-salinity intercepts yield estimates of the nitrate concentrations in the freshwater entering the two basins, $262 \pm 2 \mu\text{M}$ for Snug Harbor ($C_{\text{SH-observed}}$) and $111 \pm 2 \mu\text{M}$ for Mashapaquit Creek (C_{MC} ; ranges are the 95% confidence interval). There was no statistical difference in the nitrate concentrations calculated from 2011 and 2012 data separately, so the data were aggregated for this analysis.

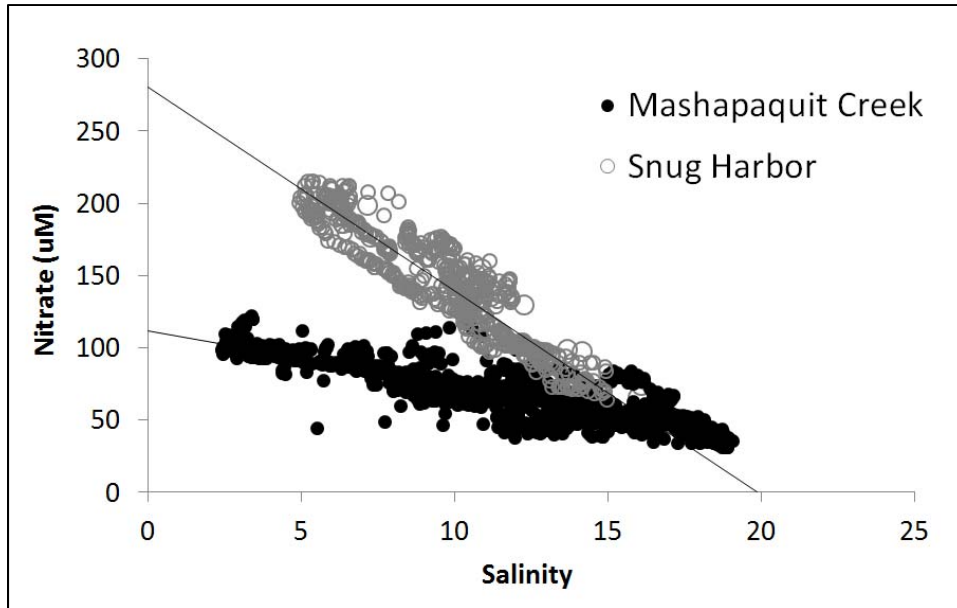


Figure 3. Nitrate concentrations as a function of salinity in Snug Harbor and Mashapaquit Creek during low-tide sampling in the winters of 2011 and 2012. The zero-salinity intercepts represent the average nitrate concentration in fresh water entering these basins.

For Mashapaquit Creek, I estimate the nitrate load from the watershed (including both the background load and the contaminated plume) from equation 2, multiplying the rate of freshwater input (Q_{MC}) by $111 \mu\text{M}$ (C_{MC}), yielding $0.19 \text{ kmol N d}^{-1}$. An estimated $0.07 \text{ kmol N d}^{-1}$ of this comes from background watershed load not associated with the contamination from the wastewater treatment facility ($B_{\text{NO}_3:\text{MC}}$; Kroeger *et al.* 2006). I therefore estimate the load to Mashapaquit Creek attributed to the wastewater facility ($\text{N Load}_{\text{plume:MC}}$) as $0.12 \text{ kmol N d}^{-1}$.

For Snug Harbor, freshwater comes from two sources; groundwater flow directly into Snug Harbor and water flow from Mashapaquit Creek. As a result, I use a weighted average to calculate C_{SH} , the concentration of nitrate directly entering Snug Harbor from groundwater:

$$C_{SH-observed} = \frac{(Q_{MC} * C_{MC}) + (Q_{SH} * C_{SH})}{(Q_{MC} + Q_{SH})} \quad (9)$$

where $C_{SH-observed}$ is the intercept from the mixing curve for Snug Harbor (260 μM). From this, I estimated the nitrate concentration in groundwater entering Snug Harbor directly (C_{SH}) as 300 μM . This is most likely a conservative estimate, since the freshwater residence time in Snug Harbor is longer than one tidal cycle (Howes *et al.* 2006), and some of the freshwater present when we made our measurements likely originated in areas of the harbor with lower nitrate inputs. From Q_{SH} and C_{SH} , I estimate the total nitrate load from the watershed to Snug Harbor (again, both from the contaminated plume and the background load) using equation 3 as 1.9 kmol N d^{-1} . An estimated 0.12 kmol N d^{-1} of this comes from the background watershed load not associated with the wastewater treatment Facility ($B_{\text{NO}_3:\text{SH}}$; Kroeger *et al.* 2006).

Consequently, I estimate the load to Snug Harbor attributed to the wastewater facility ($\text{N Load}_{\text{plume:SH}}$) as 1.8 kmol d^{-1} .

The total load to West Falmouth Harbor from the contaminated groundwater plume ($\text{N Load}_{\text{plume}}$) is the sum of the plume loads into Mashapaquit Creek and Snug Harbor ($\text{N}_{\text{plume:MC}}$ and $\text{N}_{\text{plume:SH}}$), or 1.9 kmol N d^{-1} . Summing $\text{N Load}_{\text{plume}}$, $\text{N Load}_{\text{back}}$, and $\text{N Load}_{\text{dep}}$ as in equation 1, I estimate the total nitrogen load to West Falmouth Harbor ($\text{N Load}_{\text{total}}$) as 3.0 kmol N d^{-1} , with two-thirds of this from contamination from the wastewater treatment facility. Details of temporal trends in the N load to West Falmouth Harbor are presented elsewhere (Howarth *et al.*, manuscript in preparation).

Harbor Physical Parameters and Bathymetry

Over our study period, the observed tidal range varied between 0.7m and 1.9m at neap and spring tide, respectively based on our water logger data (Figure 4). The bathymetric map generated from our survey is shown in Figure 5. The bottom of the harbor is characterized by a relatively flat, shallow plain approximately 1.3m deep at mean water level, with a deep channel running through the center as a result of past dredging. By combining the bathymetric data with the water level data I calculate a mean tidal prism of $8.0 \times 10^5 \text{ m}^3$, which is just over 50% of the total volume of water in the harbor at mean high water. The surface area of the harbor on a spring tide varies from 47 to 77 hectares, approximately a 40% change in total surface area of water. On an average tide, the difference in surface area between high and low tide is approximately 10%. Table 3 summarizes the surface area, volume, and mean depth of the harbor at different tidal stages.

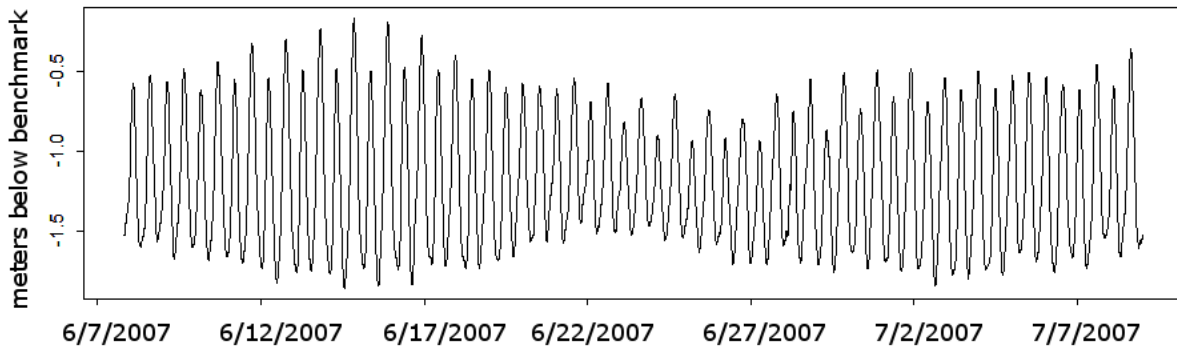


Figure 4. Variations in water level elevation over a one month timeframe in 2007. Water levels are relative to a benchmark set up on the West Falmouth Town Dock.

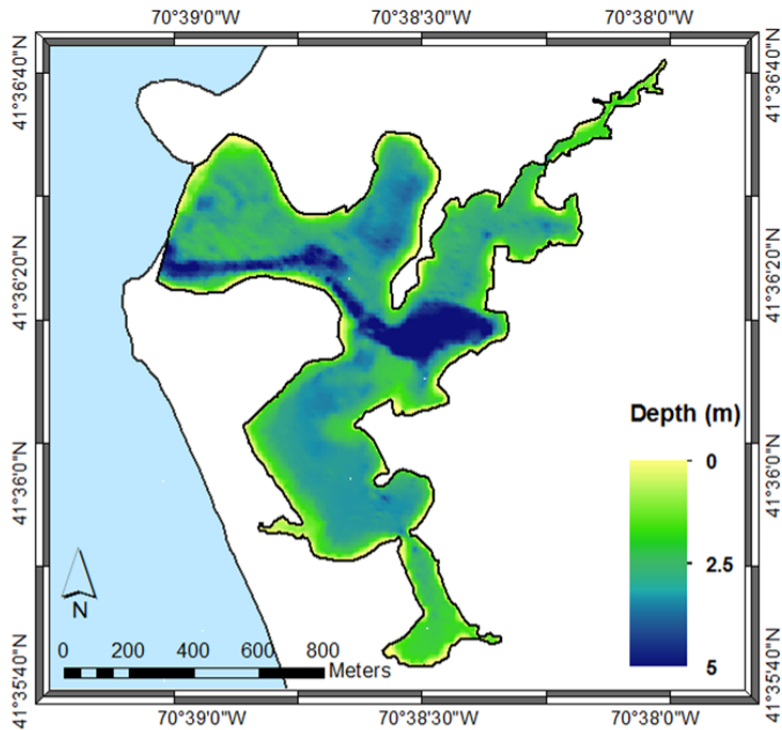


Figure 5. Bathymetric map of West Falmouth Harbor based on surveys conducted during the summer of 2008. Depths are in meters below mean higher high water.

Table 3. Physical parameters of West Falmouth Harbor based on bathymetry and water level elevation.

| Water | Water surface relative to benchmark (m) | Mean water depth (m) | Water surface area (ha) | Water volume ($\times 10^3 \text{ m}^3$) |
|-----------------|---|----------------------|-------------------------|--|
| Mean Low Water | -1.69 | 0.9 | 66.2 | 667 |
| Mean Water | -1.19 | 1.4 | 71.7 | 1,010 |
| Mean High Water | -0.56 | 2.0 | 76.1 | 1,480 |

Water Exchange

During the study period, the majority of instantaneous water exchange rates ranged from 95 to $-95 \text{ m}^3 \text{ s}^{-1}$ (positive rates are incoming water), with a median of 0. Water flux rates were normally distributed during the sampling period. I validated the instantaneous water exchange rates calculated using this method by comparing them with rate data collected by colleagues at the USGS using the index-velocity method during a one month period in 2010. The results were tightly correlated ($P < 0.0001$). Figure 6 shows the comparison between flows calculated using the volumetric change method and flows calculated by the US Geological Survey using acoustic methods over fifteen-minute intervals. Further details of the validation are available in Appendix 1 and Ganju *et al.* (2012).

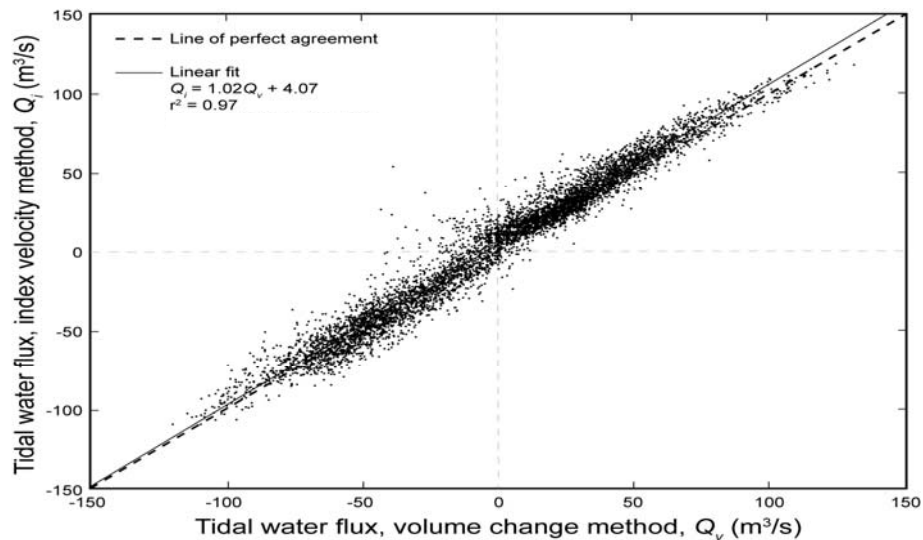


Figure 6. Comparison of a one-month sampling period in August and September 2010 over a full spring-neap cycle of water fluxes calculated using index velocity and volumetric change methods. There is good agreement between the two methods, with a 2% deviation in the slope from the 1:1 line.

Nutrient Concentrations

Nutrient concentrations at the harbor mouth show several interesting patterns when we look over all dates sampled. DIN concentrations were very low during all seasons, with an observed mean of $0.7\mu\text{M}$ and a median of $0.5\mu\text{M}$. The difference in the mean and median is a result of the skewed distribution of DIN, where concentrations are most often observed near zero with decreasing likelihood at higher concentrations (Figure 7a). Unlike DIN, TN concentrations were much higher, averaging $13.3\mu\text{M}$. On the majority of days, at least 85% of TN was composed of organic forms, and during the summer months TN was composed almost entirely of organic forms (Figure 8). There was no statistical difference in DIN concentrations among seasons sampled; however TN was slightly higher in the summer than either spring or fall (Figure 8).

SRP concentrations varied the least of all measured parameters (Figure 7c), with a mean and median of $0.6\mu\text{M}$. Unlike the relationship between DIN and TN, SRP makes up 50% on average of the TP. TP showed a mean concentration of $1.2\mu\text{M}$ and ranged from 0.1 to $2.3\mu\text{M}$ (Figure 7d). Seasonally, both SRP and TP were lower in the spring than either the summer or fall (Figure 8).

It is noteworthy that the minimum observed SRP concentration was $0.1\mu\text{M}$ and that there were no samples collected that were below the method detection limit ($0.1\mu\text{M}$). Conversely, there were 39 samples where both ammonium and nitrate were below detection limits ($0.1\mu\text{M}$ for both assays). These very low DIN concentrations are consistent with observations from other shallow systems, where rapid uptake by benthic primary producers

under N-limiting conditions results in very low levels of DIN during the growing season (Nixon *et al.* 2001; McGlathery *et al.* 2004).

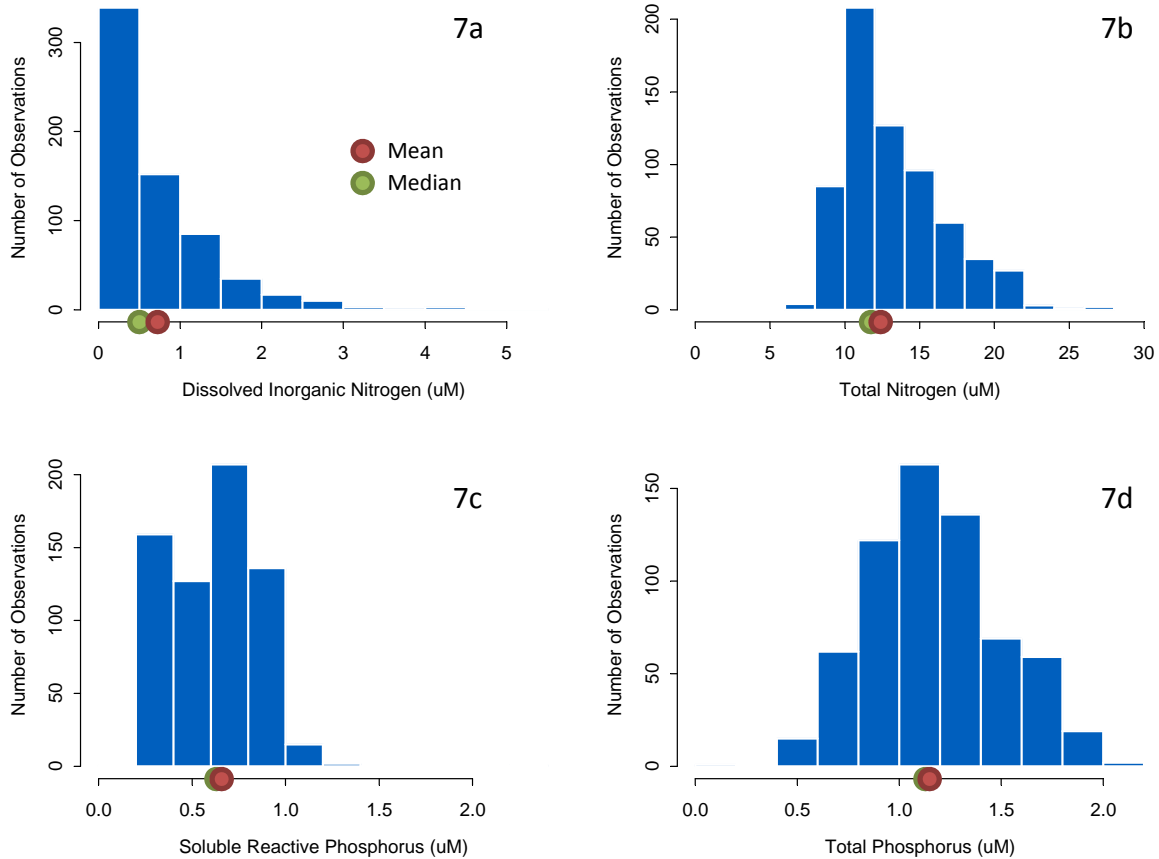


Figure 7. Histograms of observed concentrations of dissolved and total N and P over the entire observation period, encompassing spring, summer, and fall samples.

There were also interesting patterns within the set of hourly samples from an individual sampling date. On days in the spring and fall we observed fluctuations in DIN that are related to tidal stage, with concentrations peaking at the end of ebb tide (Figures 9 and 10). SRP concentrations during the spring and fall most often showed no discernible pattern (Figure 9) or

a similar pattern to the N data, with higher concentrations during ebb tide (Figure 10). During the summer, there was less hourly variation in the concentration of inorganic nutrients, and often no significant pattern with tide (Figure 11).

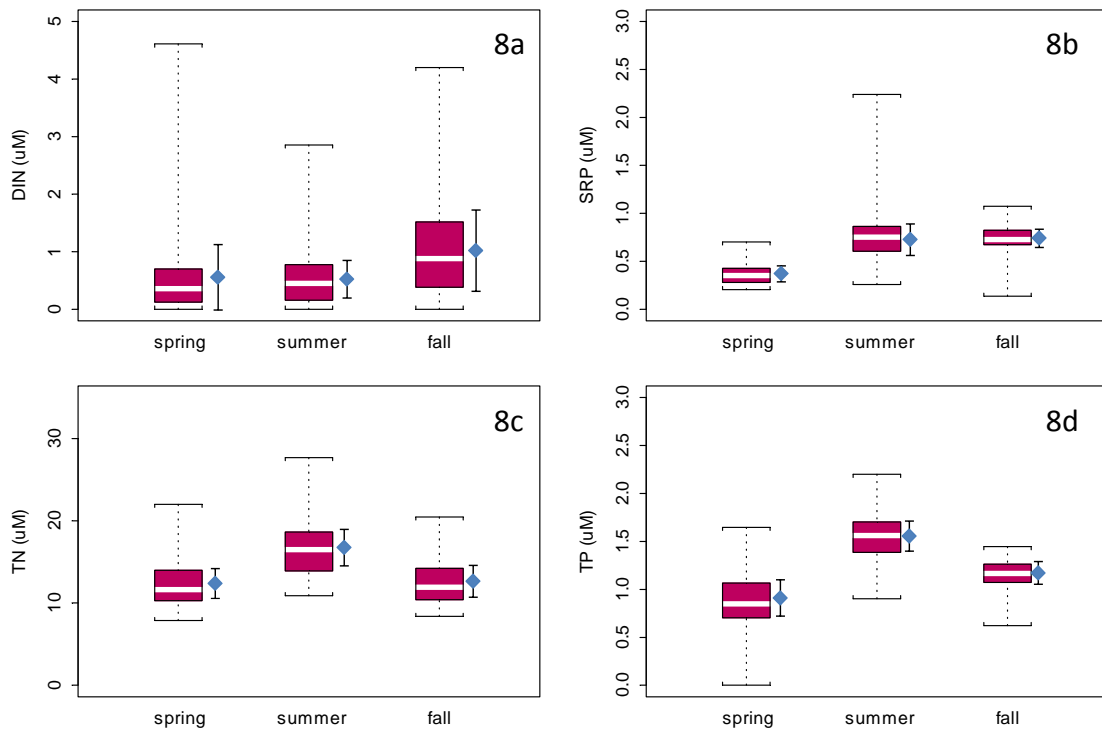


Figure 8. Boxplots showing the median (white bar), middle 50% (pink box), and full range of observations of N and P by season alongside the mean (blue diamond) and 95% confidence interval on the mean. The charts for SRP and TP have the same vertical scale, illustrating that most of the TP is inorganic. However the large difference in the scales of the N plots illustrates that most of the total N flux is organic.

Across all dates sampled, both DIN and TN concentrations were significantly and inversely correlated with water level ($P < 0.00001$). The correlation between nutrient concentration and tide was stronger in the spring and fall than in the summer, presumably due to increased biological uptake during the active growing season.

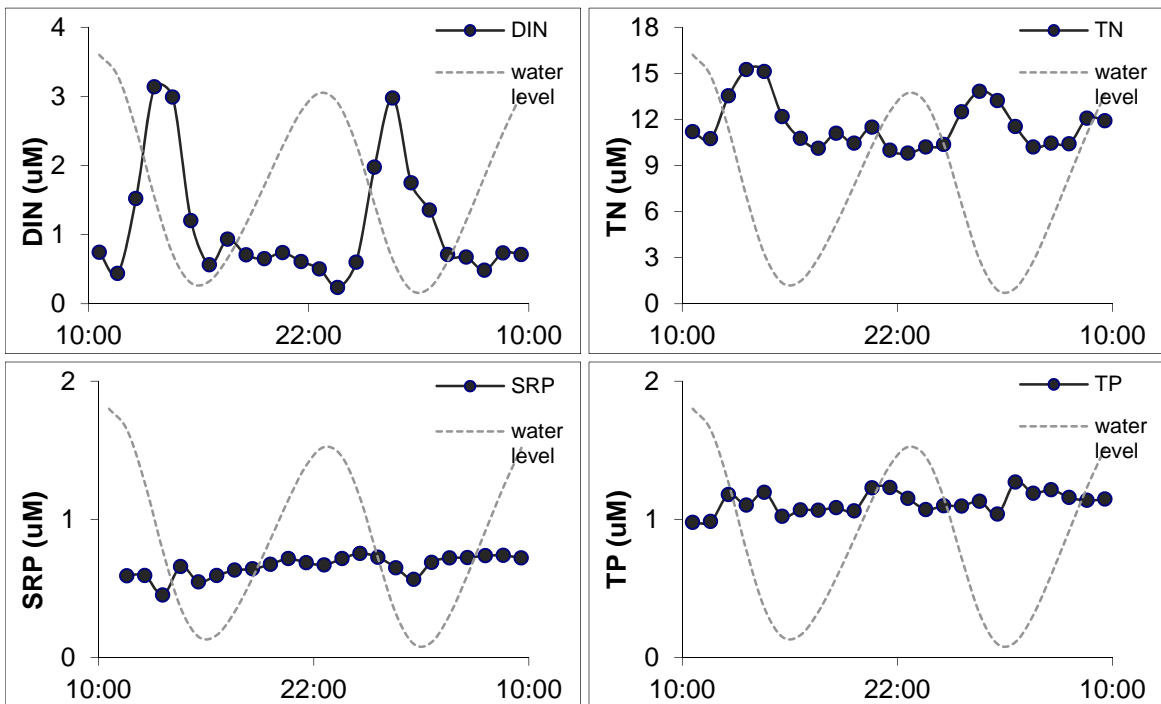


Figure 9. Patterns of nutrient concentration on September 25, 2006. The dashed lines represent water level within the harbor relative to an arbitrary datum to illustrate the tide. On this date both DIN and TN were higher when the tide was flowing out than when the tide was coming in, while there is no apparent difference in either SRP or TP between flood and ebb tides.

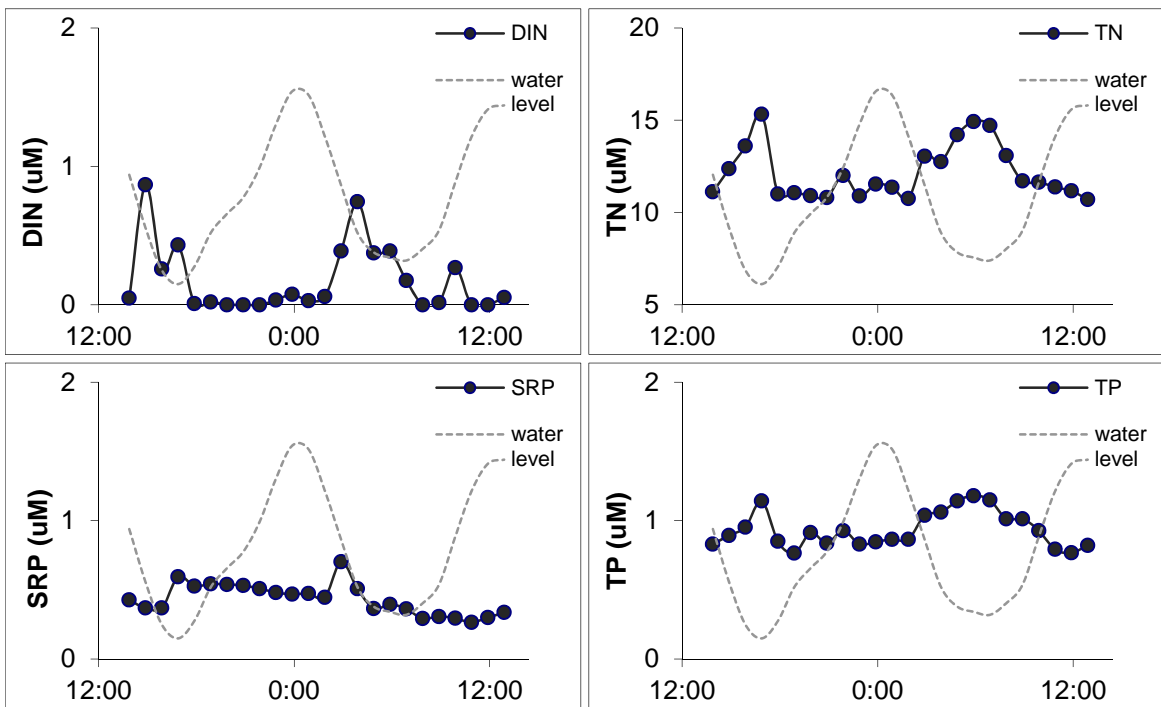


Figure 10. Patterns of nutrient concentration on May 31, 2006. The dashed lines represent the water level within the harbor relative to an arbitrary datum to illustrate the tide. On this date, there were statistically higher concentrations of DIN, TP, SRP, and TP when the tide was flowing out compared to when the tide was coming in.

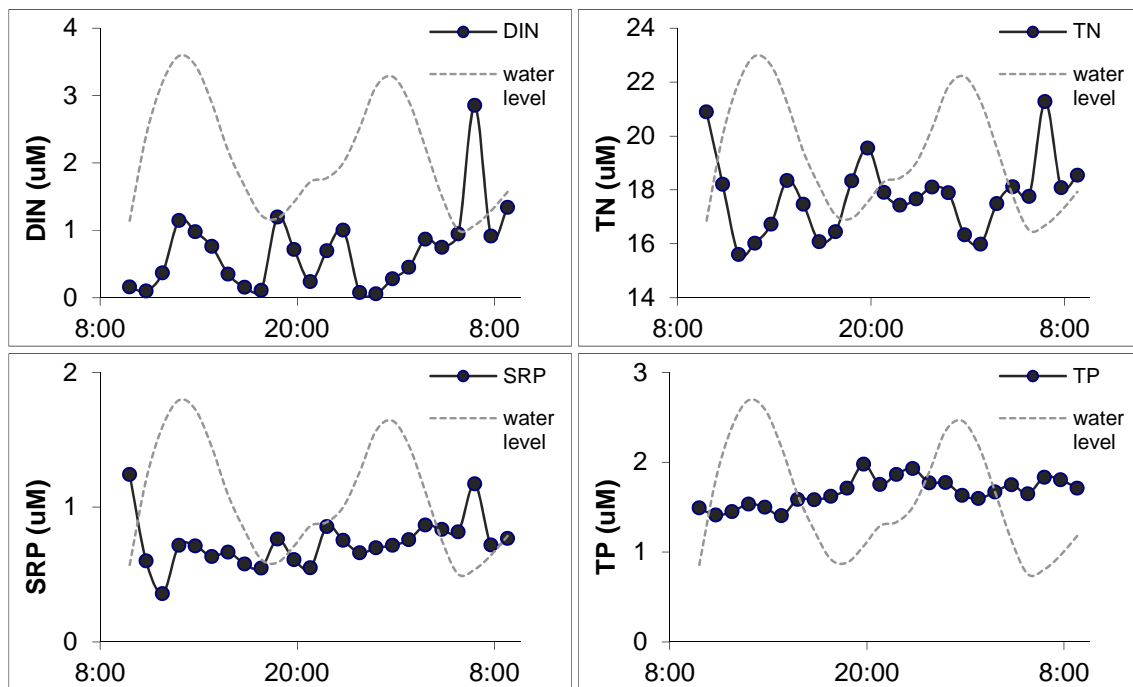


Figure 11. Patterns of nutrient concentration on July 8, 2008. The dashed lines represent the water level within the harbor relative to an arbitrary datum to illustrate the tidal level. In contrast to the previous two figures, there was no statistically significant difference in DIN or TN between flood and ebb tide.

I also compared surface and bottom DIN data from 2005 and 2006 to assess whether the system was stratified during the summer months. There was no difference in DIN between surface and bottom waters on 8 of the 11 days sampled, with no consistent pattern on the remaining three days. There was no difference between surface and bottom salinity on any of the sample days. Thus, it appears that there is no stratification present at the mouth of the harbor during the observation period, and measured N concentrations from one depth are representative of average water column concentration.

Nutrient Mass Exchange Fluxes

There is significant variation in the exchanges of TN and TP among sampling days during the same season (Figures 12 and 13), with the highest variability during the summer. Despite this variability, there are several compelling patterns in the data. During the spring and fall, all but one daily estimate for TN exchange show a net export of N from West Falmouth Harbor (Figure 12). Several of these estimates show a net export that is larger than the loading rate, suggesting that on these days there was liberation and export of N previously stored in the ecosystem. For P exchange, we generally see a net export of P during the spring (Figure 13), and on many days during the summer and fall we see a net import of TP. During the fall there is much higher variability among sampling days in the phosphorus exchange, with the days split between net import and net export.

Within individual sampling days, the error bars in Figures 12 and 13 are a representation of how sensitive the daily exchange rate is to variations in export rate over the course of the

day. Overall, there is more variation on summer days, which indicates a higher degree of variability in nutrient flux over the course of a day, presumably due to variations in primary production and consumption during the daylight hours. However, a regression analysis of tidal cycle exchange with daylight hours for 23 of the 24 days sampled did not show a statistically significant correlation ($P > 0.1$), suggesting that a confluence of factors is responsible for the variation within a day, and not simply available light.

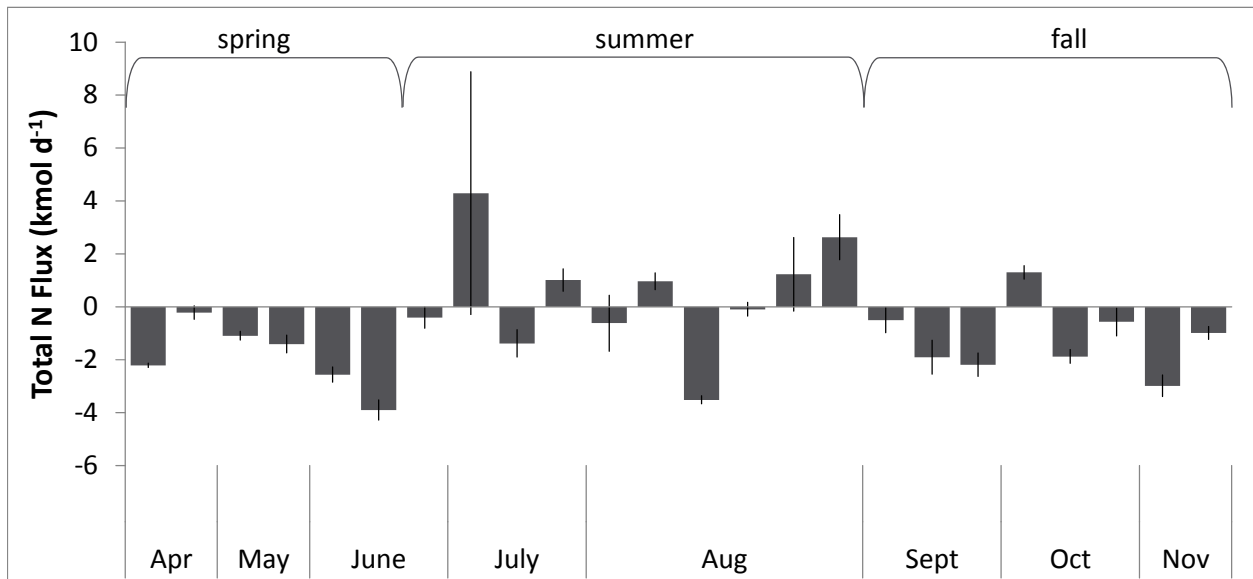


Figure 12. Daily estimates of net TN exchange calculated with the 95% confidence interval. Each bar represents the average from one sampling day. Positive values are a net influx of TN into the harbor, and negative values are a net export of TN. There is a high degree of variability between individual sample days, but there is a general trend towards net import to the harbor from coastal waters in the summer and net export in the spring and fall.

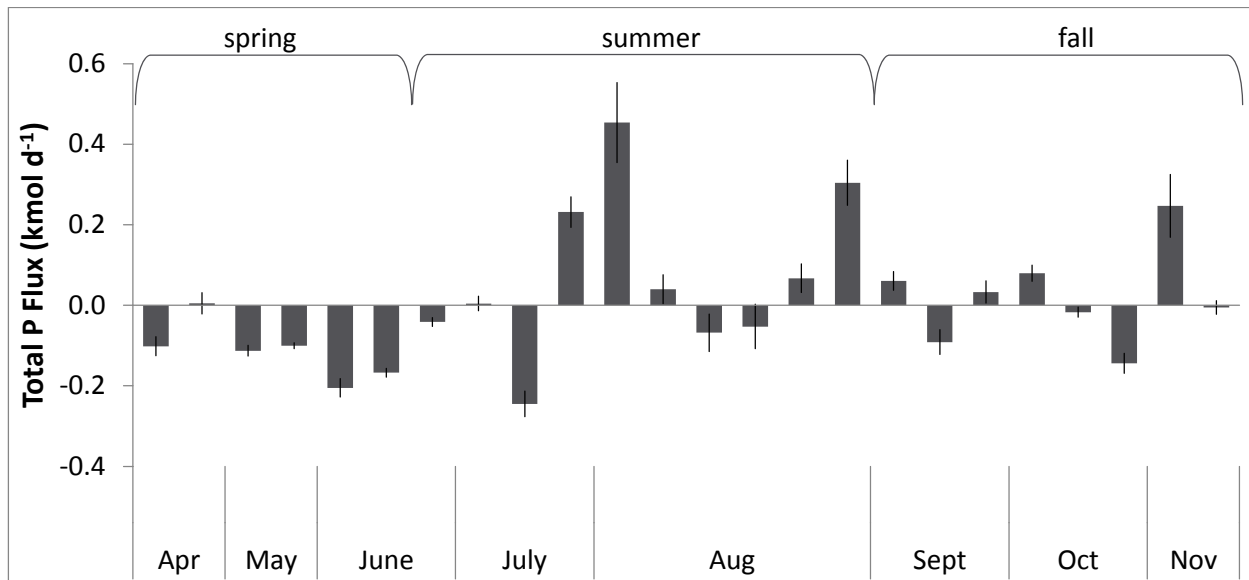


Figure 13. Daily estimates of net TP exchange with the 95% confidence interval indicated. Each bar represents the average from one sampling day. Positive values are a net import of TP into the harbor from coastal waters, and negative values are a net export of TP. There is a high degree of variability between individual sample days, but there is a general trend towards net TP export in the spring and net import in the summer and fall.

Seasonal Nutrient Exchange and Retention

The seasonally averaged exchanges of nutrients in West Falmouth Harbor (Figure 14) show interesting differences between seasons and between forms of nutrients. For all forms of N and P, there is a net export from the harbor to coastal waters during the spring and a net import to the harbor during the summer. In general, the spring and summer exchanges are composed more of organic forms of N and P than inorganic forms. The main difference is in the fall, when there is a net import of P but a net export of N, and the fluxes are composed of a larger fraction of inorganic forms than the other two seasons.

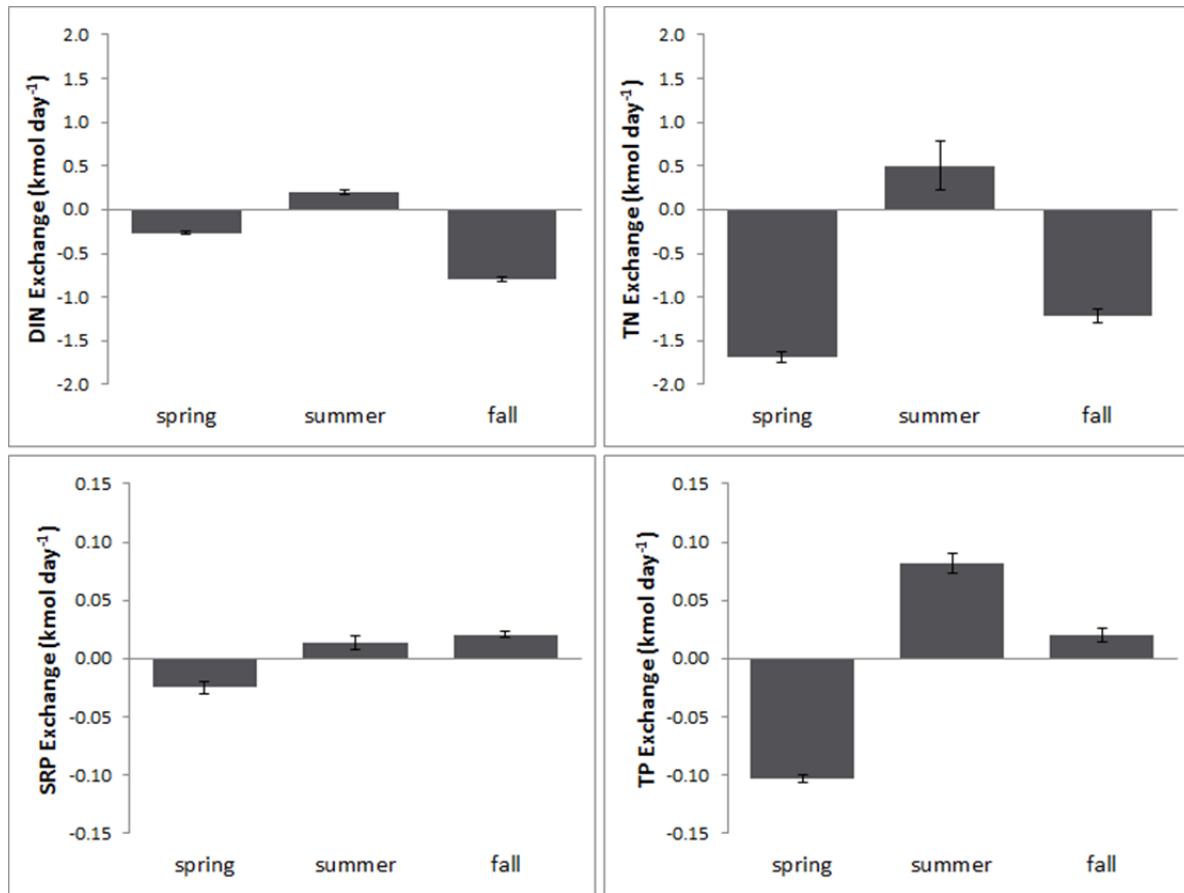


Figure 14. Seasonally averaged fluxes of DIN, TN, SRP, and TP. Positive fluxes are a net import from coastal waters. Error bars are 95% confidence intervals. Generally, we see a net import of DIN, TN, SRP, and TP during the summer, a net export in the spring, and a net export of N but net import of P in the fall.

By comparing net exchange estimates with watershed load estimates, I can examine the ability of the harbor to retain N inputs. Net retention is the sum of physical and biological processes that result in the removal of some portion of the nitrogen load to the estuary before discharge to adjacent coastal waters, and can be evaluated on both annual and seasonal bases. Depending on the time scale being examined, analysis of retention includes the net effect of temporary (seasonal) and permanent processes of N removal (including temporary storage in biomass, sedimentation, denitrification, ANAMOX, and volatilization) and N addition (nitrogen

fixation). Annual retention estimates allow us to evaluate the permanent removal of nitrogen by an estuary due to denitrification and burial in sediments (i.e. reviews by Nixon *et al.* 1996; Billen *et al.* 2011), which is important for understanding total export of nutrients to the coastal oceans. On a seasonal timescale, evaluation of retention includes the temporary storage of nutrients in biomass during the growing season, which tend to be retained on timescales of weeks to months and can be released during the fall (Risgaard-Petersen and Ottosen 2000; McGlathery *et al.* 2007).

During the summer, West Falmouth Harbor has a net import of TN from coastal waters and 100% of the watershed load is retained within the harbor. During the spring and fall, the harbor is still retaining approximately 40% and 60% of the N load, respectively. Overall, export of TN is higher in the spring than the fall, however the fraction of the export composed of DIN is much lower in the spring. Since approximately 75% of the N load is inorganic (nitrate), this low export of DIN in the spring suggests preferential assimilation of inorganic forms within the harbor. This could be a result of spring plankton blooms, where inorganic inputs are converted rapidly to organic material before export from the harbor in plankton biomass, as well as the export of organic N from the breakdown of previous years' production. In the fall, the ratio of inorganic to organic N in exports is much closer to the ratio in the N inputs, perhaps suggesting a balance of processes acting on organic and inorganic fractions within the harbor.

During the summer, however, the harbor is not only retaining the entire watershed N load, but is also importing additional N from Buzzards Bay. The summertime net N retention is therefore the sum of terrestrial and atmospheric loading ($3.0 \text{ kmol N d}^{-1}$) and import from Buzzards Bay via exchange at the mouth of the harbor ($0.4 \text{ kmol N d}^{-1}$), a total of 3.4 kmol N

d^{-1} . This is a representation of the net sum of biological uptake, loss to the atmosphere, and immobilization within the harbor in the summer months.

One mechanism for a portion of the summertime N retention is incorporation into seagrass biomass (Risgaard-Petersen & Ottosen 2000; Pedersen *et al.* 2004; McGlathery *et al.* 2007). In West Falmouth Harbor, McGlathery *et al.* (2009) estimated seagrass nitrogen assimilation rates of $13 \text{ mmol N m}^{-2} \text{ d}^{-1}$ in the Outer Harbor and $9 \text{ mmol N m}^{-2} \text{ d}^{-1}$ in Snug Harbor based on measurements of above-ground net primary productivity by the grasses in July and August and the N content in grass biomass. When I scale this areal rate using the extent of seagrass beds determined from side scan sonar surveys conducted in 2010 (Appendix 3; 16.8 ha total area), I estimate a mid-summer seagrass nitrogen assimilation rate of $2.0 \text{ kmol N d}^{-1}$ across the entire harbor. Assimilation and temporary storage of N in seagrass biomass thus can reasonably explain 60% of the net N retention of the harbor during the summer months ($3.4 \text{ kmol N d}^{-1}$); approximately 2/3 of the load from the watershed and atmosphere (3.0 kmol d^{-1}). Other mechanisms such as uptake in algae biomass (McGlathery *et al.*, unpublished data), denitrification (Giblin *et al.*, unpublished data), and burial/immobilization in sediments seem likely to be responsible for the remainder of the summertime N retention, as well as retention of additional inputs from N fixation occurring in the harbor not accounted for in these calculations (Marino *et al.*, manuscript in prep).

One striking pattern in the seasonal P exchange data is the net import of P from Buzzards Bay during both the summer and fall. Since there is a large retention of N in the summer, and the waters of Buzzards Bay have a low N:P ratio, biological demand for P beyond terrestrial loading appears to be met through this P import. The molar ratio of N:P imported

from Buzzard's Bay during the summer is approximately 6:1 (Figure 14), well below the uptake ratio for plankton and seagrasses. It also appears that this is occurring during the fall, but not in the spring.

If we assume a reasonable P loading from the watershed to the harbor of $0.05 - 0.15 \text{ kmol d}^{-1}$, (Howarth, pers. comm.), we can calculate a rough range of N:P ratios for N and P retained in the system during the spring and fall. These range from 12:1 to 27:1 (molar). Since plankton take up N and P at a ratio of approximately 16:1, and seagrasses and macro-algae at a highly variable rate commonly averaging 30:1 (Duarte 1990, 1995), the net import of P from Buzzards Bay to meet biological demand in the summer and fall is a plausible mechanism to maintaining N limitation in the harbor. In the spring we see a net export of P and a much higher ratio of N:P retained, which could be the result of remobilization of P stored in the system.

During the summer, concentrations of SRP in the water column remain fairly high throughout the tidal cycle and none of our measurements were below the detection limit, in comparison with DIN concentrations which were often below detection, particularly at low tide. This is further evidence that P supplied on the incoming tide is sufficient to meet the biological demand during the growing season and maintain N limitation despite the large terrestrial load.

Annual Nitrogen Exchange and Retention

To estimate the N retention on an annual timescale, I assume that during the winter months primary production is low and that the net N export from the harbor is equal to the inputs (3 kmol N d^{-1}). With this assumption, the annual net N exchange between West

Falmouth Harbor and Buzzards Bay averages to an export of $1.4 \text{ kmol N d}^{-1}$. This export is just less than half of the calculated N inputs from the watershed and atmosphere, and implies the processing and removal of approximately 52% of the inputs on an annual basis (Figure 15).

To compare West Falmouth Harbor with other North American and European estuaries (Figure 15), I calculated the ratio of depth:residence time ($z:\tau$) using the system residence time for Snug Harbor, which is defined as the amount of time it takes for a parcel of water in Snug Harbor to make its way out of the harbor mouth. Since the majority of the nitrogen load is entering Snug Harbor, this length of time, 5 days (Howes *et al.* 2006), represents the amount of time available for nitrogen inputs to be processed in the system and is the most relevant timescale for considering retention. West Falmouth Harbor falls slightly above the regression for other estuaries, but well within the general pattern considering the large variability seen among other estuaries.

We are fortunate in West Falmouth Harbor to have a strong spatial understanding of the sources of nitrogen. The residence time for all freshwater entering the harbor is much lower than the system residence time for Snug Harbor, since the Outer Harbor flushes very rapidly with Buzzards Bay. Without an understanding of the residence time of the parcels of high-N water, using the whole system residence time leads to a very high $z:\tau$ (over 500), and would suggest that West Falmouth Harbor is retaining significantly more of the N inputs than expected based on other systems.

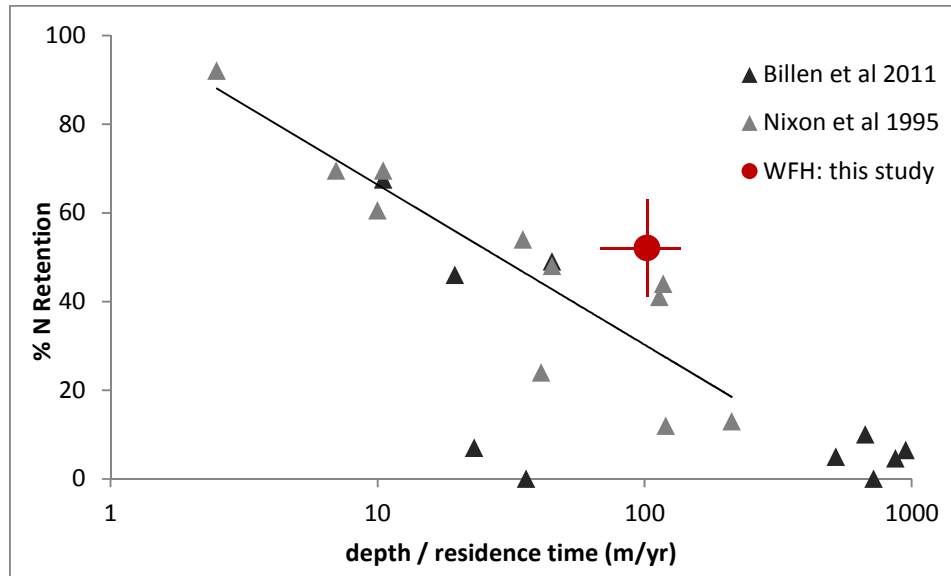


Figure 15. Relationship between N retention and the ratio of depth to residence time for North American and European estuaries, from Nixon *et al.* 1996 and Billen *et al.* 2011. The red circle is the mean annual N retention for West Falmouth Harbor, calculated using the system residence time for water entering Snug Harbor (Howes *et al.* 2006). Error bars are the 95% confidence interval for measured parameters in this study, and an assumed 20% error in residence time and terrestrial load.

The majority of systems in the Nixon *et al.* (1996) and Billen *et al.* (2011) reviews are deeper systems than West Falmouth Harbor, with primary productivity dominated by short-lived phytoplankton which cannot retain nitrogen for long periods. In shallower systems, light penetrates to the sediment surface and allows the proliferation of high-productivity benthic plants, macro-algae, and benthic micro-algae. In addition to the large changes in seasonal retention dynamics by these species described in the previous section, this large benthic autotrophic community also has the potential to increase annual N retention directly through incorporation of N into biological material and enhanced burial. Although turnover rates for plant and algal tissue vary, nutrients assimilated by benthic plant communities tend to be retained on timescales of weeks to months (McGlathery *et al.* 2007). During that time, there is the potential for enhancement of long-term N retention processes resulting from the effects of

plant metabolism on sediment oxygen and nutrient and organic matter concentrations that influence N burial (McGlathery *et al.* 2007), although the exact mechanisms of this enhancement are not yet well studied.

CONCLUSION

West Falmouth Harbor has provided a unique opportunity to study the effects of a dramatically increased terrestrial N load without an increase in P load. Despite the large N load, the harbor is able to retain the entire terrestrial N load during the summer, and imports additional N from the coastal waters of Buzzards Bay. Phosphorus import during the summer from Buzzard's Bay is also high, providing a source of P in addition to the terrestrial P load to meet the summertime biological demand stimulated by high N inputs. The N:P ratio imported from coastal waters during the summer is low (6:1, molar ratio), supporting the conclusion that P imported from nearshore waters is sufficient to maintain N limitation during peak growing season. On an annual scale, West Falmouth Harbor is retaining about half of the nitrogen inputs from the watershed and atmosphere, which is comparable to other Northeastern United States and European estuaries with a similar ratio of depth to residence time.

There have been several recent papers suggesting that under conditions of high nitrogen loading, primary production in an estuary can switch from N limitation to P limitation (EPA/SAB 2008; Conley *et al.* 2009; Paerl 2009, Howarth *et al.* 2011). In West Falmouth Harbor, it does not appear that this situation has occurred. The phosphorus input from Buzzards Bay during the growing season is sufficient to maintain nitrogen limiting conditions at the current rate of terrestrial loading.

APPENDIX 1:

Spatial Modeling in Estuaries: Using Ordinary Kriging to Estimate

Tidal Water Flux in West Falmouth Harbor

Typically, hydrodynamic modeling is used in conjunction with chemical analyses to study flows of nutrients into and out of estuarine systems. In this study, I evaluate the use of an alternative method of calculating water flow, which uses basin bathymetry and water level observations to calculate water fluxes. I collect a bathymetric data set for West Falmouth Harbor and interpolate a continuous surface using ordinary kriging, which allows me to construct a network of statistically optimal predictions and standard error estimates at a grid of unobserved locations. I calculate water fluxes from this bathymetry and compare these fluxes to those computed using the index-velocity method to test the accuracy of the predictions, and show that the two methods agree closely on estimates during a one month period. For simple systems such as West Falmouth Harbor, which meet a specific set of hydrologic assumptions, this much simpler method of determining water fluxes is a viable option for long-term nutrient studies.

METHODS

Bathymetric data collection

I collected depth soundings in three ways. I collected the majority of the data with the assistance of CR Environmental Consulting, using a single beam echo sounder from a 16' aluminum survey vessel and Hypack-4.3A Gold hydrographic survey software. I installed a Global Water 16W tide gauge centrally within the harbor to provide water level corrections to the survey data. Horizontal positioning was accomplished using a Trimble AgGPS 132 12-channel differential geographical positioning system (DGPS) with OmniStar satellite based differential corrections to obtain sub-meter accuracy. This method was used to gather data in water depths greater than two feet. I gathered data from the shallower regions of the harbor manually using the DGPS and a meter stick while physically walking the boundary of the site. I also digitized the high tide line from aerial photographs and ground-truthed using the DGPS combined with a handheld PC. The high tide line was assigned the water level of monthly average highest high tide, based on observations in the field. A total of approximately 122,000 depth sounding locations were collected (Figure A1-1) and used in this analysis. I computed Euclidean distances between sites using the easting and northing coordinates from data gathered in the Massachusetts State Plane Mainland – Meters projection.

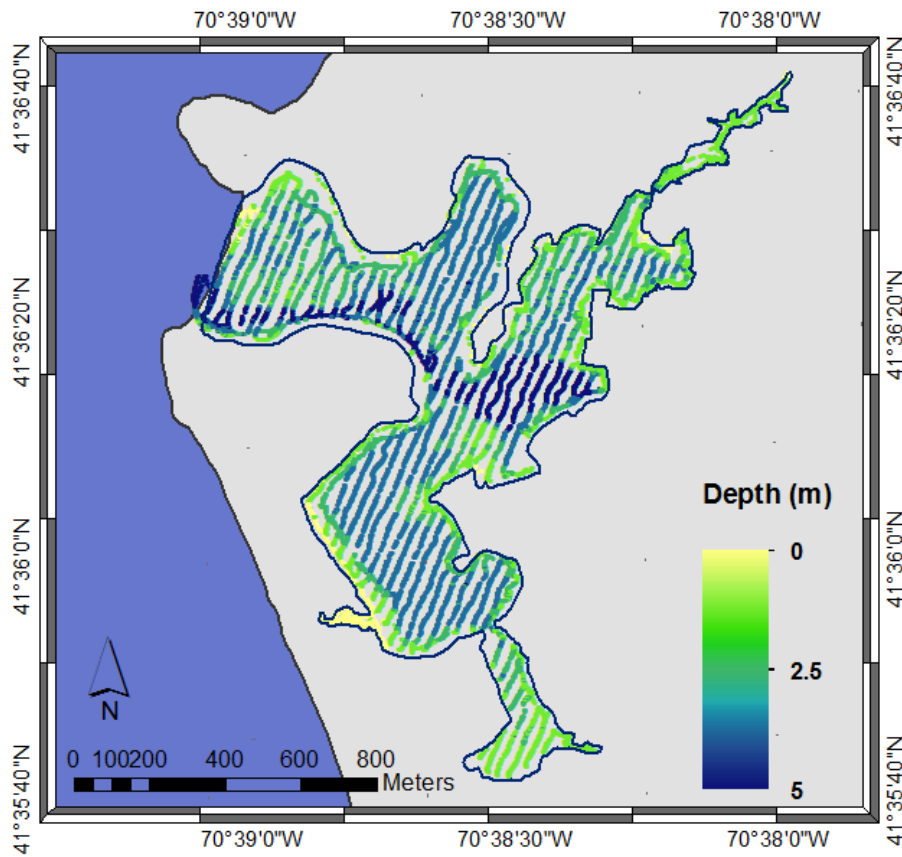


Figure A1–1. Map of bathymetric data used as model input. Points are color coded based on depth in meters below a local benchmark. The mouth of the harbor where water exchanges with Buzzards Bay is near the northwest corner of the harbor.

Spatial Interpolation

The objective of this spatial analysis is to predict the depth $\hat{Z}(s_0)$ at a grid of unsampled sites (s_0) based on our network of collected bathymetry data $Z(s_1), \dots, Z(s_{122000})$. Kriging is a popular approach to spatial prediction due to the stability of the predictions under varying model assumptions (Cressie and Zimmerman 1992). For this dataset, I used ordinary kriging as the best linear unbiased estimator. This method is appropriate for a data set where the mean is unknown but the spatial autocorrelation of the data is known through the covariance matrix.

The kriging predictor is written as a linear function of the observed data at the network of original sample sites (Cressie and Zimmerman 1992):

$$\hat{Z}(s^*) = \lambda' Z \quad (1)$$

$$\lambda' = \left(k + 1 \frac{(1 - 1' K^{-1} k)}{1' K^{-1} 1} \right) K^{-1} \quad (2)$$

where $\lambda_1 \dots \lambda_n$ are chosen to minimize the mean squared prediction error given by:

$$E(\hat{Z}(s_0) - Z(s_0))^2 \quad (3)$$

I carried out the kriging interpolations in two separate software packages using the same exponential variogram parameters. First, I used ESRI ArcGIS 9.2 and the Geostatistical Analyst package to evaluate depth over a 5m spatial grid. I also used the spatial module within Tibco-Spotfire S-Plus, where I estimated depth at 6056 locations separated by approximately 11m in the x direction and 13m in the y direction. The resulting interpolated surfaces from these two programs were compared and found to be statistically indistinguishable on multiple scales.

I validated the interpolated data by predicting the values for a separate set of validation points, taken in transects at right angles to the original data collection (Figure A1-2). The prediction residual sum of squares was calculated from the standard errors of these predictions according to the following equation:

$$RSS = \sum_{i=1}^n \{Z_i - \hat{Z}_i\}^2 \quad (4)$$

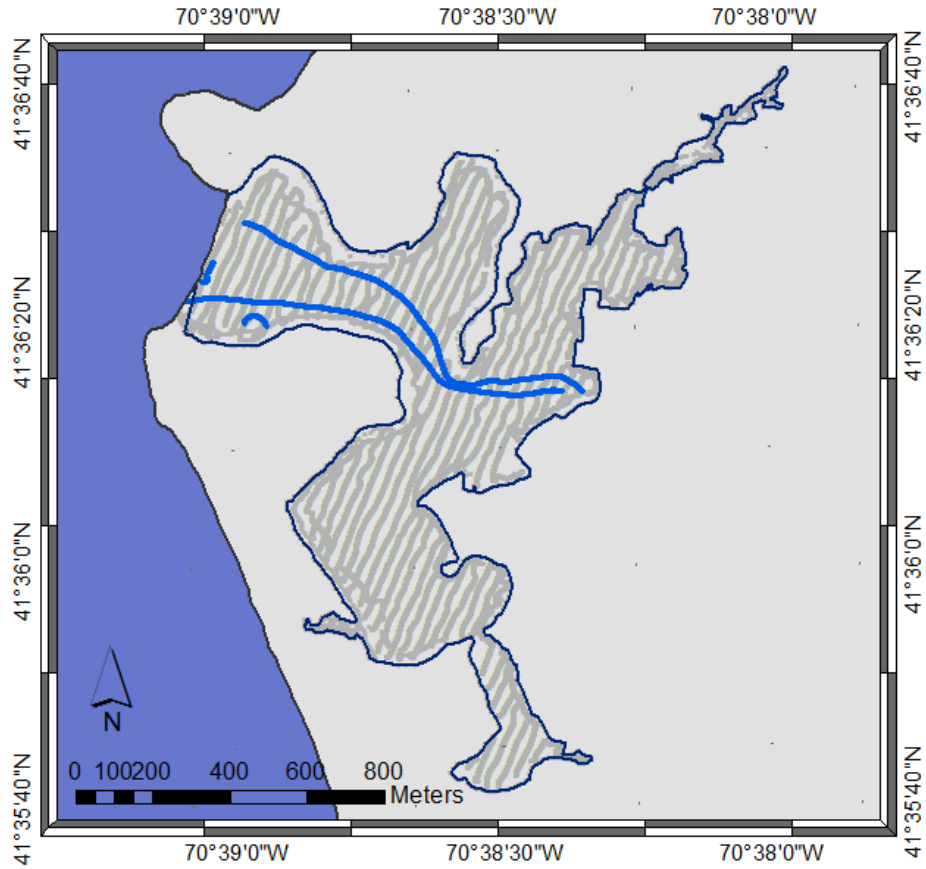


Figure A1–2. Locations of validation points are shown in blue. Gray points are the original observations used to create the interpolation model.

Volume Estimation

I calculated the volume of the estuary at a given water level from the interpolated surface by summing the volume over each prediction point at a given water level in the estuary according to the following equation:

$$V(WL) = \sum_{i=1}^n \{A * (\hat{Z}_i - WL)\} \tag{5}$$

where i is the set of prediction locations within the estuary that are submerged at a given tide level, A is the area over which each prediction applies, \hat{Z} is the predicted depth of point i in meters relative to the benchmark, and WL is the water level of interest, also in units of meters relative to the benchmark. I calculated the volume at a set of water levels that span the maximum range of water levels observed over a six month period, and used these volumes to determine a linear equation to predict volume based on water level. This equation is of the form:

$$V = X\beta + \varepsilon \quad (6)$$

where V is the volume of the estuary the water levels of interest, X is the design matrix of water levels of interest, and β is the coefficient matrix determined from predictions from equation 6 (Kutner *et al.* 2004). The standard error for a given volume estimate was made under the assumption that the standard errors for individual kriged predictions were independent, and the standard error for the volume was calculated as the sum of the squared errors for the predictions used to calculate the volume.

Water Flux Calculation – Volumetric Change Method

I calculate water exchange between West Falmouth Harbor and Buzzards Bay using a volumetric change model and water budget for the harbor. Inputs to the harbor come from precipitation and groundwater, and exports via evaporation and net tidal exchange. I model the change in harbor volume over time as:

$$\frac{dV}{dt} = Q_v + P + G - E \quad (7)$$

where dV/dt is the rate of volume change in $\text{m}^3 \text{s}^{-1}$, Q_v is the water exchange at the mouth (positive values are inflowing tide), G is groundwater flux, P is precipitation, and E is evaporation. Since Q is several orders of magnitude greater than P , G , and E at any given time, this model reduces to:

$$\frac{dV}{dt} = Q_v \quad (8)$$

Since the harbor can be modeled as a standing wave with minimal lag between embayments (Howes *et al.* 2006), I can calculate the volume of water within the harbor from bathymetry and water level measurements made at a central location and use this to calculate water flux rates. I collected water level measurements at five minute intervals from spring through fall using a Global Water WL16 vented, pressure and temperature compensated water level logger (accurate to 0.009m). From the water level data, I calculated a continuous record of harbor volume during the study period, and calculated instantaneous rates of water exchange (Q_v) over my periods of interest using the following equation:

$$Q_v = \frac{V_2 - V_1}{t_2 - t_1} \quad (9)$$

Water Flux Calculation – Index Velocity Method

The index velocity method uses acoustic data to measure water discharge rates through confined channels, and has been the standard method used by the USGS to measure discharge from streams and estuaries since the mid-1990's (Gotvald and Oberg, 2009). The method uses a deployed acoustic doppler current profiler (ADCP) to continuously monitor water velocity, which is calibrated using the index-velocity rating empirically developed for the study site by surveying the full cross-sectional velocity over a complete tidal cycle (Ruhl and Simpson, 2005). A Nortek Aquadopp ADCP was deployed in the channel at the mouth of West Falmouth Harbor for approximately one month in 2010 by colleagues at the US Geological Survey. They periodically determined the cross-sectionally averaged channel water velocity and channel cross-sectional area at the mouth, and used these values to calibrate the continuous record from the ADCP. Further detail is described in Ganju *et al.* (2012). These measurements were taken concurrently with flux estimates using the volumetric change method, to evaluate the accuracy of our water fluxes from 2005-2009.

RESULTS

Model Fit and Predictions – Bathymetry Interpolation

A variogram is a function which describes the degree of spatial dependence within a dataset, and is defined as the variance of the difference between values at pairs of locations within a sampling grid (Cressie and Zimmerman 1992). Figure A-3 shows the empirical variogram and variogram fit for the set of depth observations used to calculate the bathymetry

of West Falmouth Harbor. The variogram model was fit to the first eight distance bins of data, where spatial correlation is the strongest. The range of the resulting variogram is approximately 100m. For the experimental variogram, this range represents approximately 1/3 of the range of spatial correlation in the data (Kaluzny *et al.* 1998), suggesting that points in this dataset within 300m of each other are spatially correlated.

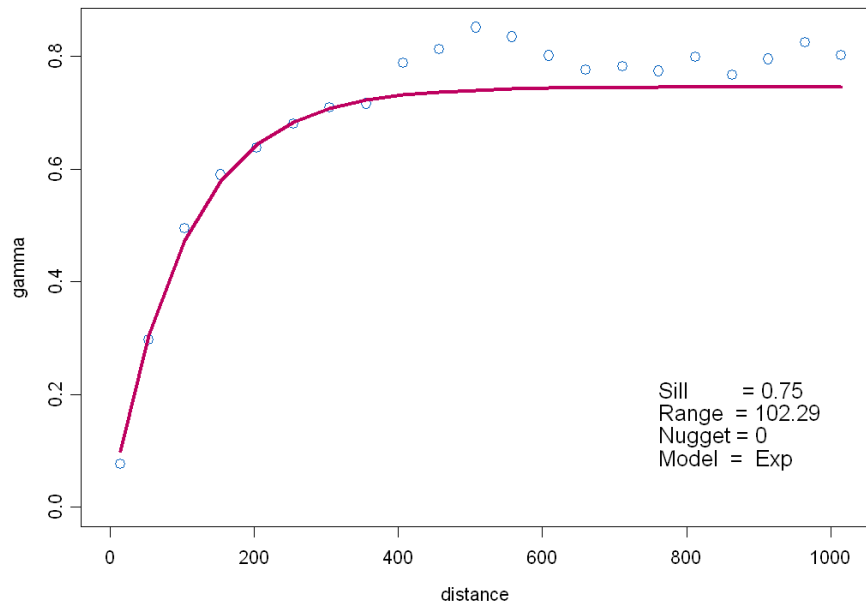


Figure A1-3. Exponential semivariogram fit by weighted least squares in S-Plus using the variogram.fit function.

Figure A1-4 shows the resulting kriged predictions over the specified regular sampling grid. It shows a deep channel running roughly east to west through the center of the harbor, reflecting an artificially maintained channel for vessel passage. It also reflects generally shallower depths in the farther inland reaches of the estuary to the north and south. The standard error surface from the kriging analysis (Figure A1-5) reflects the method of data collection, where there are stripes of data with lower error estimates immediately surrounding

the transects of data collection and larger standard errors between these lines and in less densely sampled regions close to shore.

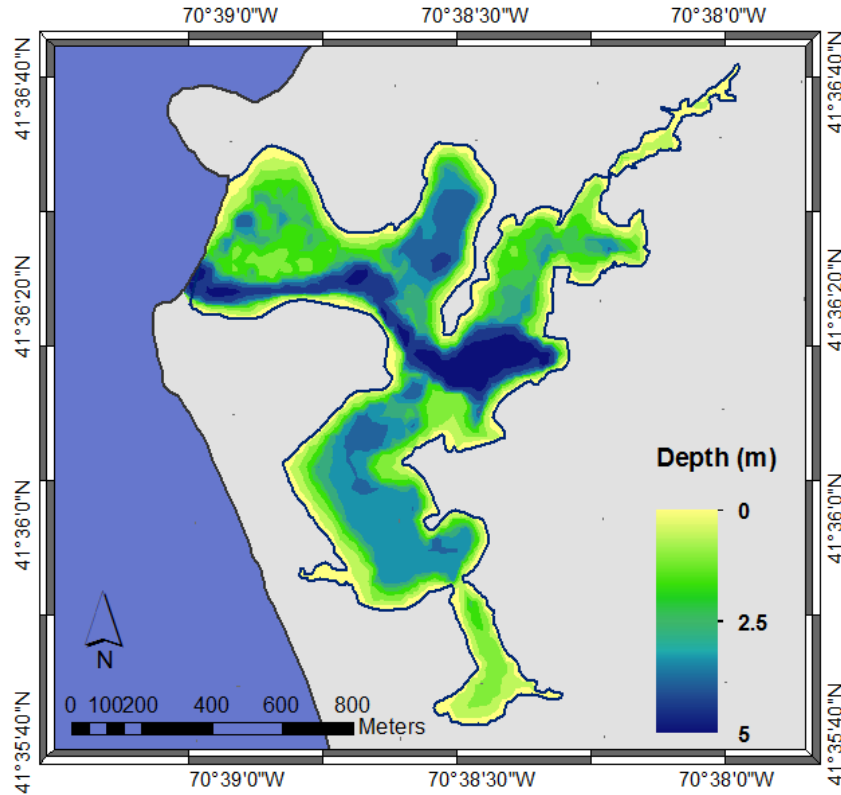


Figure A1-4. Kriged surface of the estuary at a regular grid of prediction locations. Values are meters below mean higher high water.

The predicted depths \hat{Z} for the validation points ranged from -4.7 to -2.0 meters, which is representative of the range over the majority of the estuary. The residuals generated from comparing the modeled results to the original were centered around zero, and are heavily weighted close to zero, reflecting the majority of the points with residuals less than 0.25m (Figures A1-6 and A1-7). The RSS for the validation data was 20.3 with 254 degrees of freedom, yielding a residual mean square of 0.08 .

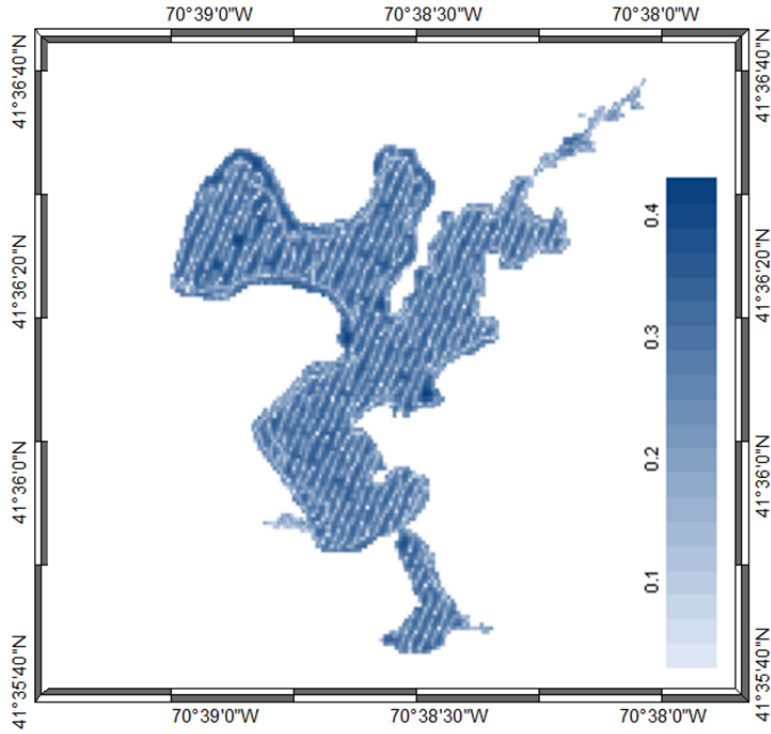


Figure A1–5. Standard error surface resulting from kriging analysis. Standard error units are meters.

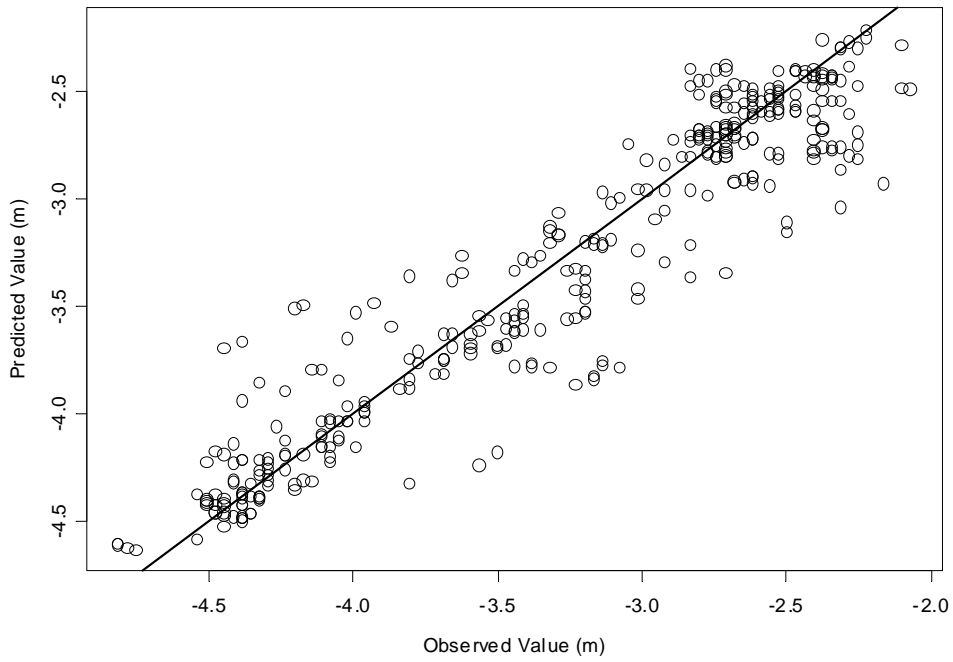


Figure A1–6. Comparison of predicted values of harbor depth from the kriged model compared to the observed depth values for the validation data transect. The line is the 1:1 line.

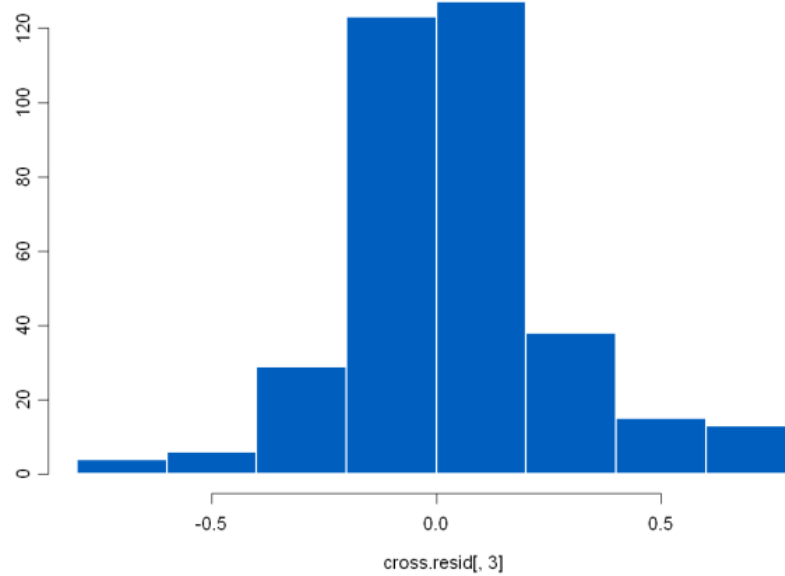


Figure A1-7. Histogram showing the residuals for the validation dataset, which represent the difference between the calculated depth and the observed depth in the field.

Volume and Standard Error

The relationship between volume and water level show a tight correlation ($p < 0.0001$) (Figure A1-8). This suggests that in the range of water levels observed at this site a simple linear regression based on water level is a good predictor of the volume as estimated from the kriging analysis. The standard error of the bathymetric surface at a selection of water levels is shown in Table A-1. The range of standard errors calculated using the sum of squared errors method ranged from 13% to 23% over the range of average low to high tide. However, when computing change in volume over time, only the error over portions of the harbor that are exposed at low tide needs to be accounted for, since the error cancels out for areas that remain submerged. On an average tidal cycle, the surface area of the harbor changes by 10%. So while

the percent error in the entire bathymetric surface can be as high as 23%, the error calculated over a mean tidal cycle is approximately 3%.

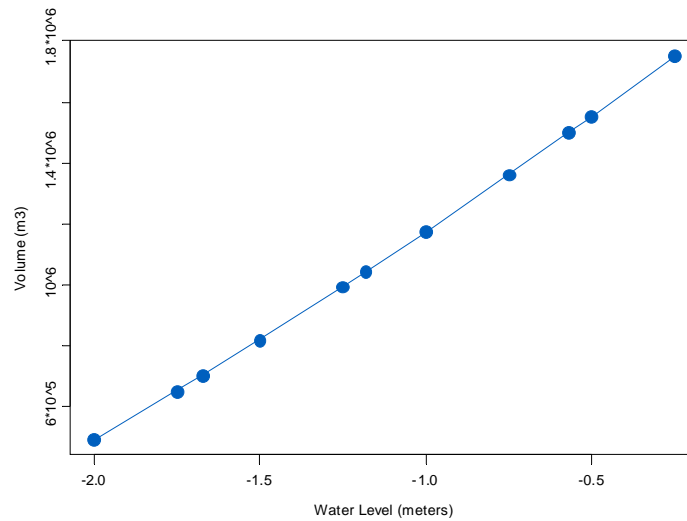


Figure A1-8. Relationship between water level and volume of the harbor, with prediction line from polynomial linear model fit, second order. The coefficients of β_0 - β_2 for this analysis are $\beta_0=1,957,000$, $\beta_1=833,600$, and $\beta_2=49,800$.

| Table A1-1. Comparison of volume, SSE, and SE as a percent of the predicted volume at different water levels. | | | | |
|---|---------------------------------|--------------------------|-----------------------|---------------|
| Tide Stage | Water Level (m below benchmark) | Volume (m ³) | SSE (m ³) | Percent Error |
| mean low tide | -1.67 | 703,000 | 165,000 | 23% |
| average tide | -1.18 | 1,043,000 | 178,000 | 17% |
| mean high tide | -0.57 | 1,499,000 | 191,000 | 13% |

Continuous Tidal Water Fluxes

A continuous record of tidal flux in West Falmouth Harbor was calculated over summertime periods in 2005 – 2010 using the volumetric change method. Peak flows were approximately $130 \text{ m}^3 \text{ s}^{-1}$ during spring tides. There is very good agreement between these water fluxes when calculated using either the volumetric or index-velocity methods when compared over a period during August, 2010 (Figure A-9). A direct comparison of the two methods has $P < 0.0001$, an intercept indistinguishable from zero (Figure A-10), and normally distributed residuals with the majority of the differences in the instantaneous rates less than $2 \text{ m}^3 \text{ s}^{-1}$ (Figure A-11).

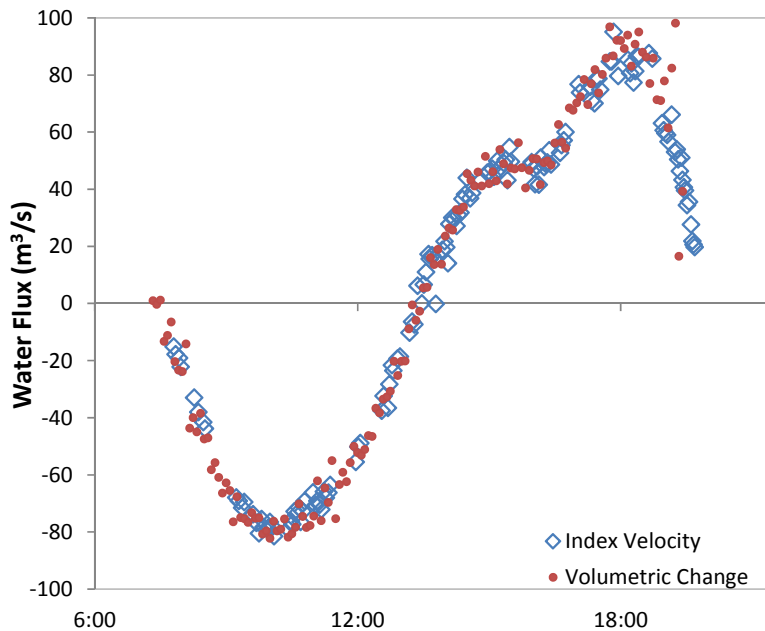


Figure A1-9. Comparison of water fluxes using the index velocity method and volumetric change method during a full tidal cycle during a spring tide on August 9, 2010.

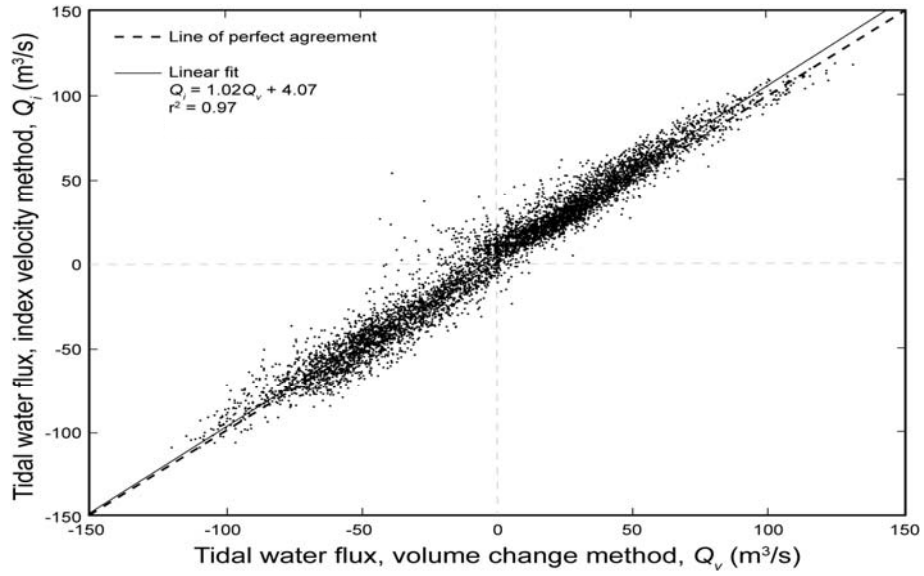


Figure A1–10. Comparison of a one-month sampling period in August and September 2010 over a full spring-neap cycle of water fluxes calculated using index velocity and volumetric change methods.

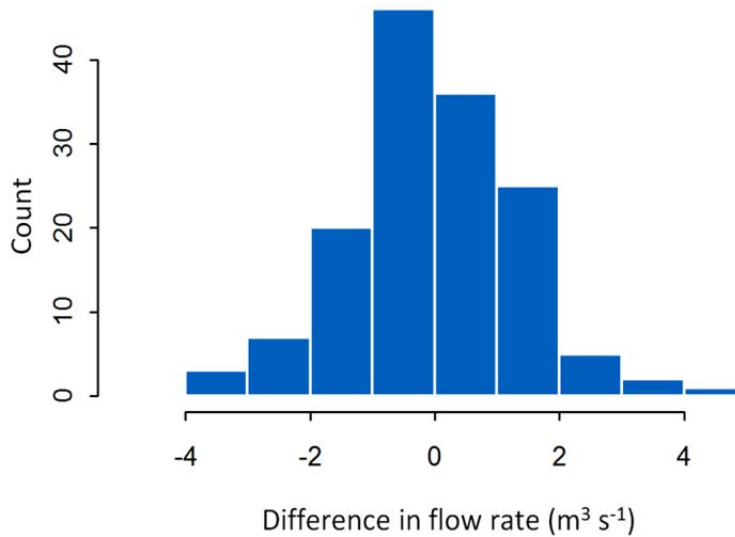


Figure A1–11. Residuals of the flow rate comparison between the index-velocity method and the volumetric change method on 8/9/10.

DISCUSSION

The results from this analysis demonstrate that ordinary kriging can be used to interpolate a set of spatial data into a continuous grid representing the basin shape of West Falmouth Harbor with a reasonable degree of accuracy (13-23% error in volume across the entire estuarine area depending on water level).

With the sophistication of computing technology over the last decade, methods of spatial interpolation have been increasingly looked to as a way to turn discrete sets of samples into a more continuous prediction for a study area. Several recently published papers have examined the effect of different variogram estimates and distance metric estimates on the results from kriging analysis within estuaries (i.e. Little *et al.* 1997; Rathbun 1998). These studies have shown that even in estuaries with highly convoluted shapes, using different distance metrics, variogram forms, and models (universal vs. ordinary kriging) with the kriging algorithm yields only small improvements in prediction accuracy when applied to sets of depth data observations at the low sampling densities of past decades. Currently, with the high data densities made possible using acoustic methods, differences in variogram form and model used yield even smaller differences in prediction accuracy, leading to easily obtainable accurate representations of the bathymetry of estuarine systems.

Acoustic methods of determining instantaneous water fluxes through confined channels have been the standard in recent years (Simpson and Bland, 2000; Ruhl and Simpson, 2005). However these methods require deployment and maintenance of an ADCP during periods when the flow is to be calculated, which can be expensive and is not feasible for many systems due to constraints on budget and manpower for maintenance. The volumetric change method for

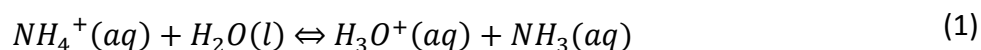
determining instantaneous water fluxes yields accurate results in West Falmouth Harbor, and likely has applicability to other systems that satisfy the necessary criteria (short residence time, spatially uniform water level at any given time). This method only requires specialized equipment up-front to determine an accurate bathymetry (assuming there are not large substrate changes occurring in the system). Beyond this, the maintenance of a water level logger is the only requirement to calculate water fluxes, and can be done from shore with no boat support. Because of the low annual maintenance requirement, it is very cost-effective to obtain a continuous record of water flux using this method.

APPENDIX 2:

Estimation of the Importance of Ammonia Volatilization in Nitrogen Flux Estimates in West Falmouth Harbor

Volatilization of nitrogen compounds, primarily ammonia, is an important mechanism for nitrogen loss in many natural systems with conditions that favor volatilization, including sites with high pH and high ambient ammonium concentrations (i.e. Bowden, 1986). In aquatic systems, studies at some sites have shown a net system loss of ammonia through atmospheric exchange, including the northern Pacific and Atlantic Oceans (Quinn *et al.* 1988, Zhuang and Huebert, 1996) as well as the Arabian Sea during part of the year (Gibb *et al.* 1999). However, these losses are of low magnitude relative to other nitrogen fluxes in the system, and the majority of studies in lakes and coastal systems have found that ammonia loss due to volatilization is inconsequential as a nitrogen flux when compared with the dominant fluxes in the system (i.e. Koop-Jakobsen, 2003; Dudel and Kohl 1992). The exceptions are systems where eutrophication or other conditions have caused an increase in site pH levels and/or surface water ammonium concentrations (i.e. Larsen *et al.* 2001; Murphy and Brownlee, 1981).

Ammonia is highly soluble, and when dissolved in water is present in an equilibrium state between the ionic form and dissolved gaseous form (Equation A2-1).



The equilibrium constant for the above reaction (K_a) is 5.6×10^{-10} ($pK_a=9.25$). This means that at a pH of 9.25, ammonium ions and dissolved ammonia gas are present in equal concentrations.

Since most marine systems away from highly productive coastal areas have a pH of approximately 8.1, the amount of ammonia gas present is about 10% of the total dissolved ammonia concentration.

In West Falmouth Harbor, high levels of primary productivity can lead to large fluctuations in daily pH values due to the diurnal fluctuations in dissolved oxygen and carbon dioxide (Howarth *et al.* MS in prep). These swings in pH values led me to examine the potential role of volatilization in the nitrogen budget.

For seven dates between 2006 and 2010 we have simultaneous measurements of ammonium ion concentration (at hourly intervals) and pH (at 20-minute intervals) at two sites within the harbor (Outer Harbor and Inner Harbor) as well as data from two dates in the Southern Basin. Since there is much less variation in the ammonium concentration than the pH data, I extrapolated the ammonium data to a 20-minute interval using a linear interpolation, and calculated ammonia gas concentrations in the water at each 20-minute interval over an approximately 24-hour period for each date based on the relationship shown in following equation

$$[NH_3] = \frac{[NH_4^+] * K_a}{[H^+]} \quad (2)$$

where $[NH_3]$ is the dissolved ammonia concentration, $[NH_4^+]$ is the dissolved ammonium ion concentration, K_a is the dissociation constant for ammonia ($10^{-9.25}$), and $[H^+]$ is the hydrogen ion concentration, which can also be represented as 10^{-pH} .

Since the system is well-mixed, I assumed that that solute concentration was homogeneous throughout the water column. Ammonium concentrations observed during all measurements ranged from 0 μ M to 2.4 μ M, with a mean of 0.2 μ M for the outer portion of the harbor and 0.4 μ M for the inner regions of the harbor, and pH values ranged from 7.0 to 8.2.

The transfer of gas across the air-water interface can be summarized by the following equation:

$$F = k [C_w - C_{air}] \quad (3)$$

where F is the flux of gas in mol m⁻² day⁻¹, k is the transfer coefficient (m d⁻¹), and [C_w-C_{air}] is the gradient in concentration of the gas between the solution (C_w) and the concentration in equilibrium with the atmosphere (C_{air}) in mol m⁻³. For this calculation, I assumed that the atmospheric ammonia concentration was zero, to look at the maximum rates of gas exchange. To derive the transfer coefficient, I used the relationship from Marino and Howarth (1993) for oxygen exchange as a function of wind speed in similar systems (equation A2-4), and corrected for the difference in diffusivity between ammonia and oxygen (equation A2-5).

$$k_{O_2} = e^{(1.09 + 0.249 * u)} \quad (4)$$

$$k_{NH_3} = k_{O_2} \left(\frac{Sc_{NH_3}}{Sc_{O_2}} \right)^{-1/2} \quad (5)$$

In the above equations, k_{O₂} is the transfer coefficient for oxygen (m d⁻¹), u is the wind speed (m s⁻¹), and k_{NH₃} is the transfer coefficient for ammonia. The ratio of transfer coefficients is proportional to the ratio of Schmidt numbers (Sc) for each gas, which are based on the ratio of

water viscosity to molecular diffusivity of the gas. I used the Schmidt ratio exponent of $\frac{1}{2}$, which is applicable for wavy, unbroken water surfaces with no bubble entrainment (Ledwell 1984, Jahne *et al.* 1987, Watson *et al.* 1991) and should be applicable during non-storm conditions.

For each day, I calculated the flux (F) of ammonia gas on a 20-minute interval at each site, and then integrated to get the total daily ammonia flux in $\text{mol m}^{-2} \text{d}^{-1}$. I applied the rate for each site to the surface area of that part of the harbor at mean water, and then added the basins together to get total flux from the harbor. The table below (Table A2-1) shows the dates where data on ammonium and pH were available, and the atmospheric exchange rates (F) calculated for each of these days. Additionally, I took the maximum daily rates calculated for each region of the harbor (Outer, Inner, and South Basin) and added them to get a potential maximum observed rate. Based on these calculations, ammonia volatilization is responsible for the loss of less than 1% of terrestrial inputs (3.0 kmol d^{-1}) even when we consider the maximum rates calculated for all areas of the harbor. This leads us to conclude that under current conditions, ammonia volatilization is not a significant nitrogen loss process in the system.

| Table A2-1. Summary of ammonia volatilization rates for individual summertime days sampled, as well as the rate calculated by combining data from individual sites on days with maximum volatilization rates. | |
|---|-------------------------------|
| Sampling Date | NH ₃ flux (kmol/d) |
| 8/16/2006 | 0.006 |
| 6/26/2007 | 0.006 |
| 8/21/2007 | 0.011 |
| 7/22/2008 | 0.016 |
| 8/18/2008 | 0.006 |
| 7/28/2009 | 0.007 |
| 7/27/2010 | 0.004 |
| max combined | 0.019 |

Given that the pH observed in West Falmouth Harbor is often greater than 8.0 with a maximum observed around 8.2 (Howarth *et al.* MS in prep), I used the previous approach to explore what conditions of ammonia concentration and pH in the harbor could result in ammonia volatilization that would constitute a significant loss of the terrestrial load. I ran simulations with increased ambient ammonium concentrations to see at what point the volatilization became significant. Figure A2-1 shows the effect of increasing ammonium concentration while using the same wind speed, temperature, and pH dynamics as used in the calculations of current volatilization. This simulation shows that at concentrations only a few micromolar over the ambient concentrations observed during my 2006-2008 water samplings, the loss to volatilization becomes a non-trivial component of the nitrogen budget. These higher ammonium concentrations would be plausible if primary production in the harbor were to

become limited by a factor other than nitrogen availability, resulting in a lower uptake rate of nitrogen during the summer. This could potentially allow ambient nitrogen concentrations to increase to levels necessary for significant volatilization.

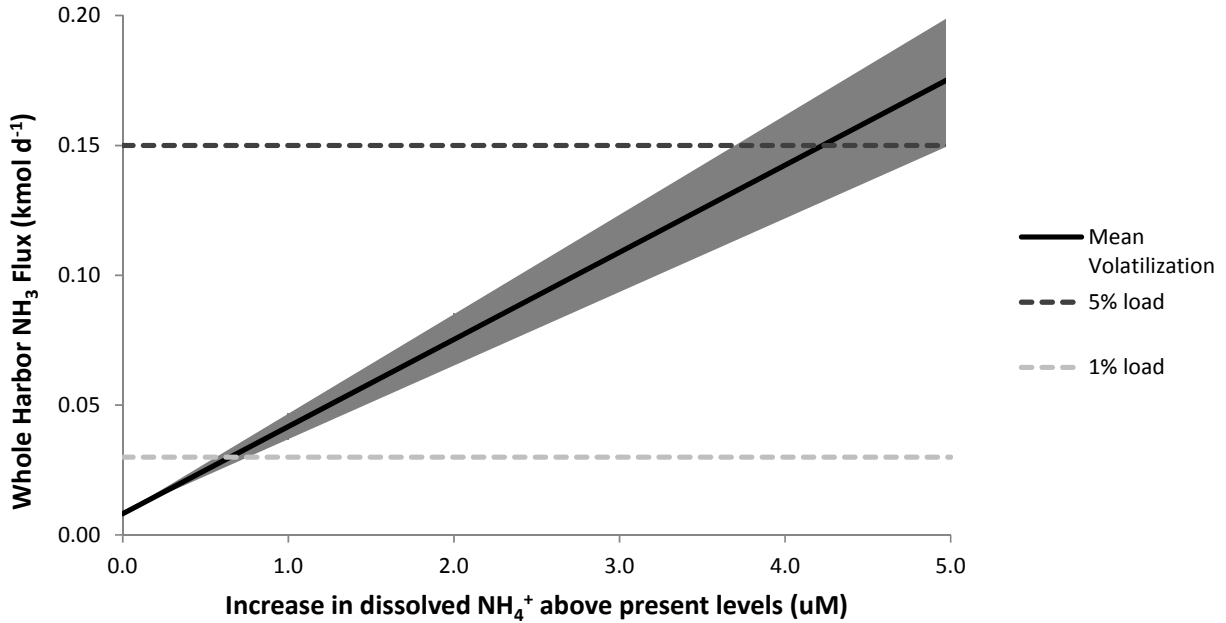


Figure A2-1. Change in ammonia volatilization rates as dissolved ammonium concentrations within the harbor increase above present levels (present average: 0.3 μM), based on the mean volatilization rate calculated in Table A2-1. Shaded area indicates 95% confidence intervals. The dotted lines represent fractions of estimated current terrestrial N load (3.0 kmol d⁻¹). At an approximately 4 μM increase in ambient concentrations over those observed in my study, volatilization could result in the loss of 5% of the total terrestrial load.

APPENDIX 3:

Using Side Scan Sonar for Seagrass Distribution in West Falmouth Harbor

METHODS

To determine the areal extent of seagrass beds in West Falmouth Harbor, I conducted surveys during early May 2010 using side scan sonar with the assistance of CR Environmental, Inc. We acquired acoustic data along survey transects which were spaced to provide 100% coverage of the harbor bottom in the survey area. We used an Edgetech, Inc. 4100-P system consisting of an Edgetech 272-TD towfish interfaced to a topside processor running Chesapeake Technology, Inc. SonarWiz5 acquisition software to collect the data, using a 500-kHz frequency and 25 meter range (per channel) to accommodate the shallow water depths over most of the harbor. Horizontal positions were provided by a Trimble AgGPS 132 with U.S. Coast Guard beacon differential corrections. A draft sonar mosaic was produced in real-time during the survey to ensure adequate coverage and to allow preliminary identification of bed extent for ground-truthing. I used an underwater video system consisting of a SeaDrop 950 and SeaViewer LCD display to identify bottom type at pre-determined coordinates to provide calibration data for image processing. The three primary bottom types observed during the survey (sand, organic/silt/clay, seagrass bed) had clearly differentiable sonar signatures. I further verified the presence/absence of seagrass at 10 locations per basin of the harbor the following week using scuba to provide additional validation points for the interpreted sonar data.

Eli Perrone from CR Environmental conducted preliminary processing using SonarWiz5 software to adjust for signal attenuation through the water, georeference the data, and export georeferenced imagery to ESRI ArcGIS 10.0 for classification. Due to the small size of the study site, I classified the imagery manually in ArcGIS. I identified bed areas by using the video drops to identify the visual signature of seagrass beds, then hand-digitized seagrass polygons on an high definition monitor. Figure 1 shows an example of one area that contained both organic bare sediment (light areas) and seagrass bed (dark mottled areas). A bed is operationally defined in this analysis as a location with a high enough seagrass shoot density to be distinguishable using sonar technology. Sparse areas with just a few plants per square meter will not be discernible on the side scan image. However, since these areas are a very small fraction of the total plants in the harbor, the error from their exclusion should be negligible

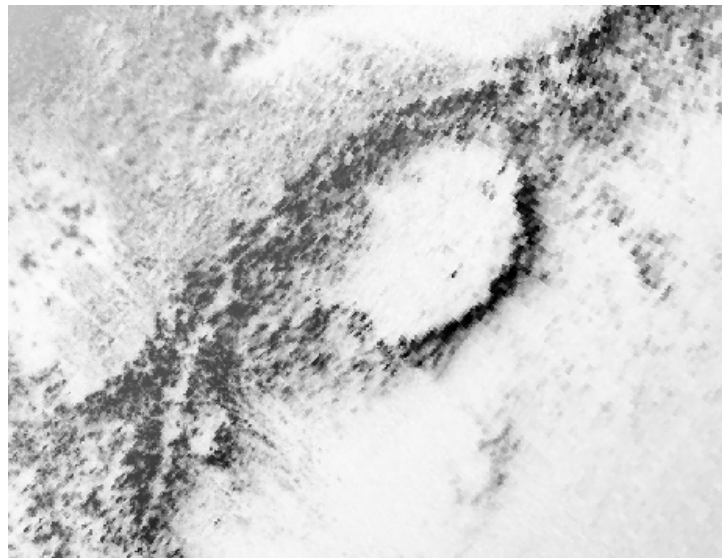


Figure A3-1. In this image, the edge of the seagrass bed is clearly visible, as well as the bare patch around a mooring. In the upper left corner are small rocks, and the lower right corner is loss of signal due to downward sloping bathymetry.

RESULTS AND DISCUSSION

The seagrass extent in West Falmouth Harbor from my analysis of the side scan sonar images is shown in Figure 2. As of this survey in May 2010, just under 25% of the mid-tide area of West Falmouth Harbor contained seagrass beds. The total extent is 16.8ha of seagrass bed with the majority (14.2ha) present in the outer portions of the harbor (which includes our Outer Harbor site, as well as the adjacent basin which is hydrologically similar) and 2.6 ha in the inner portion of the harbor (Snug Harbor). The image clearly delineates key features, such as the bare patches around moorings, the sandy bare areas near the mouth of the harbor, and the detritus beds in the northern part of the Outer Harbor where there are only occasional live seagrass shoots.

To my knowledge, this is the first sonar survey for seagrass extent that has been conducted in West Falmouth Harbor. Historically, the Massachusetts Department of Environmental Protection (MA DEP) has estimated seagrass extent along the MA coastline using a combination of analysis of aerial photography and field verification (Costello and Kenworthy, 2011). The three most recent DEP surveys (1995, 2001, and 2006) are shown in Figure 3, alongside our results for 2010. The bed extents from the DEP surveys are similar across the three years analyzed, with a few interesting trends. Overall, the extent of the main seagrass bed in the outer portion of the harbor is decreasing, as seagrass in the southeast area of the bed has died back over the past 15 years.

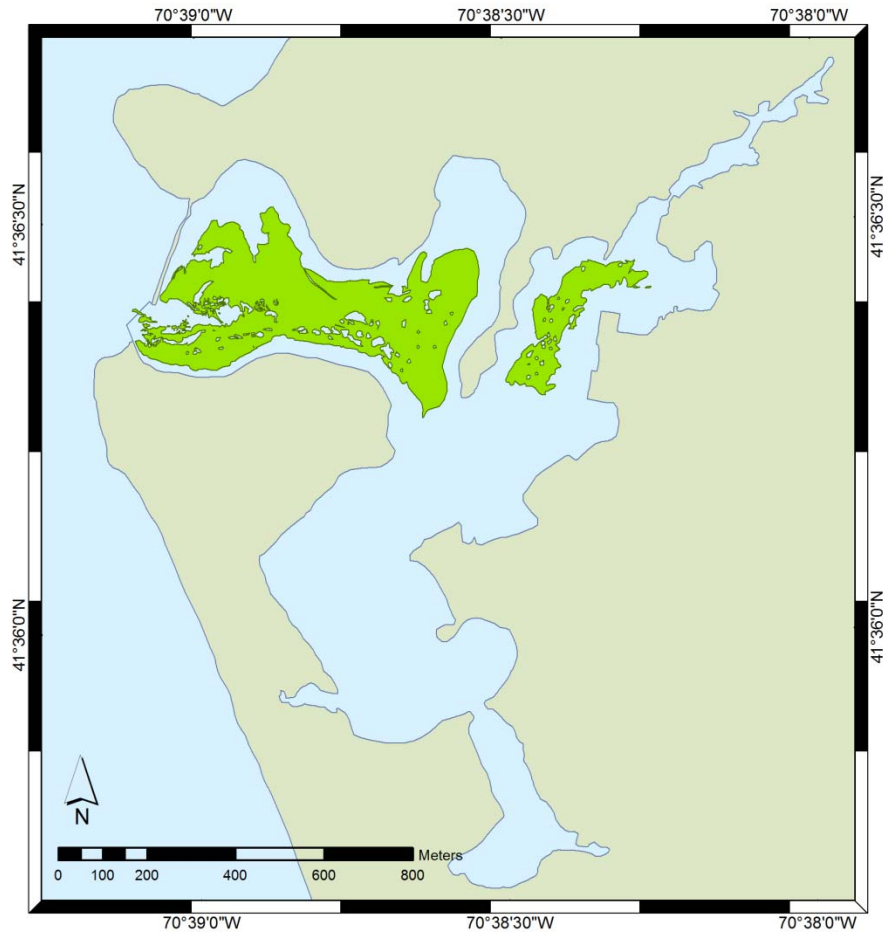


Figure A3–2. The seagrass extent resulting from side scan analysis for 2010, illustrating the wide distribution through the outer portions of the harbor and limited extent in the inner portions of the harbor. Overall, 16.8ha of the harbor contains seagrass beds as of spring, 2010.

While the distribution and extent of seagrass appears similar between the past DEP extent estimates and my 2010 estimate (Table 1), the total area of seagrass bed I calculate is significantly lower due to several key differences. The largest discrepancy between the DEP data and mine is in the northern portion of the Outer Harbor. This approximately 1.2 ha area has been classified by the DEP as an area where seagrass is present in 1995-2006, however our field observations since 2005 have consistently found a large detritus field with the occasional

seagrass shoot and a large population of mid-summer macroalgae. Also, the DEP analyses appear to consistently underestimate the size of the bare area just inside the mouth of the harbor. Thus, while my 2010 analysis of total seagrass extent using sonar data is approximately 15% lower than the DEP's most recent published estimate in 2006 (19.4ha, Costello and Kenworthy, 2011), my estimate is consistent with recent historical patterns and with in-situ field observations of the presence or absence of seagrass in particular areas. The finer detail we are able to obtain with the side scan sonar technique coupled with video and scuba surveys provides a more accurate accounting of current seagrass bed extent for use in scaling seagrass process measurements such as primary production and nitrogen fixation.

| Table A3–1. Comparison of seagrass areas estimated from side scan sonar surveys (this study; 2010) with previous areal estimates from surveys conducted by the MA DEP (1995, 2001, 2006). | | | |
|---|-------------------------------|-------------------------------|-----------------------------------|
| Year | Outer Harbor Area (ha) | Inner Harbor Area (ha) | Total Seagrass Extent (ha) |
| 1995 | 19.1 | 2.3 | 21.4 |
| 2001 | 17.0 | 2.0 | 19.0 |
| 2006 | 17.4 | 2.0 | 19.4 |
| 2010 | 14.2 | 2.6 | 16.8 |

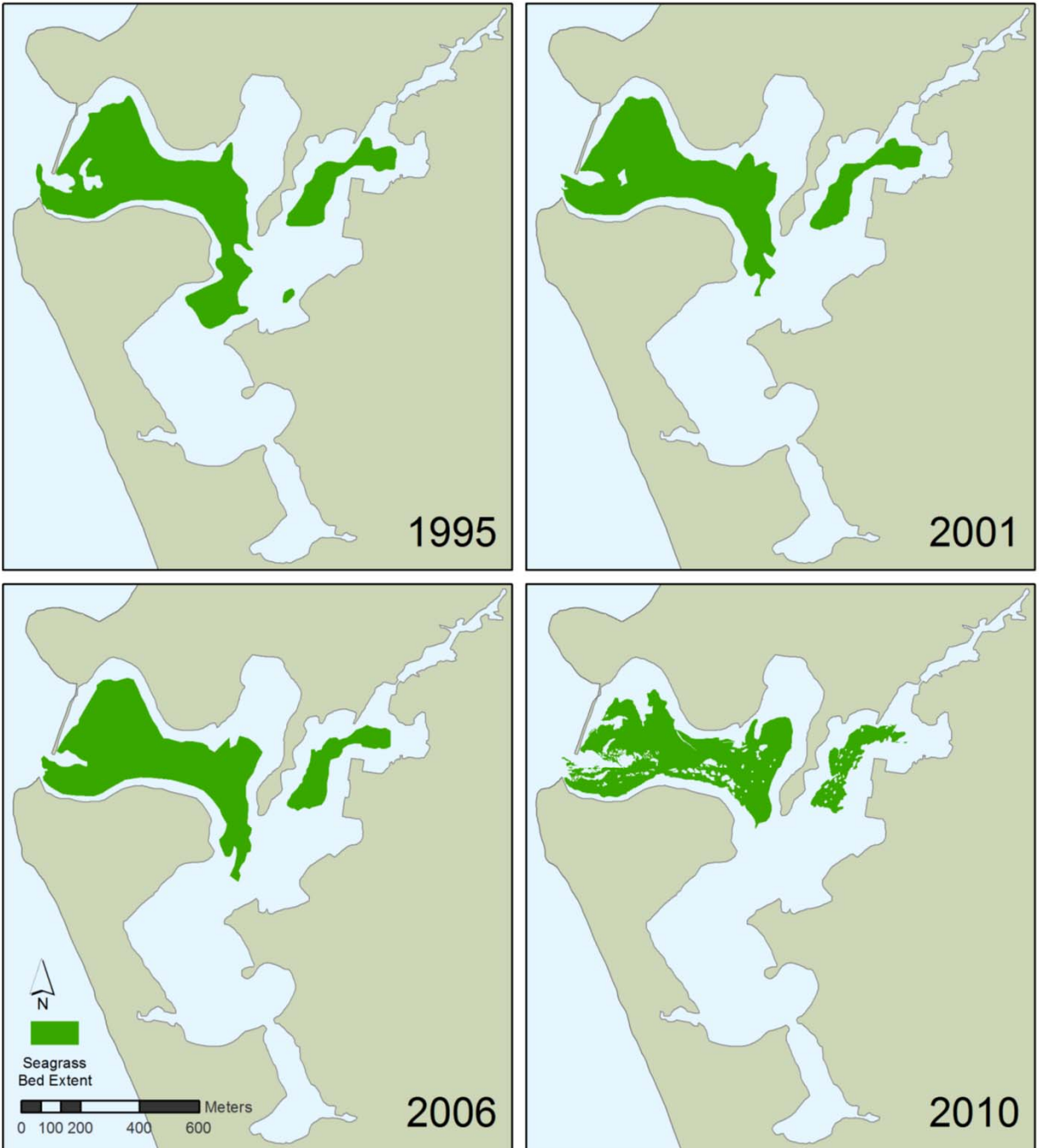


Figure A3-3. The difference in seagrass extent over time as mapped by the Department of Environmental Protection in 1995, 2001, and 2006 based on aerial photography in comparison with my 2010 seagrass extent mapped from side scan sonar imagery. While the majority of the distribution appears similar over time, there is much more detail in the sonar survey. (DEP seagrass extent data courtesy of the Office of Geographic Information (MassGIS), Commonwealth of Massachusetts, Information Technology Division).

REFERENCES

- Billen, G., M. Silvestre, B. Grizzetti, A. Leip, J. Garnier, M. Voss, R. Howarth, F. Bouraoui, H. Behrendt, A. Lepisto, P. Kortelainen, P. Johnes, C. Curtis, C. Humborg, E. Smedberg, O. Kaste, R. Ganeshram, A. Beusen, & C. Lancelot. 2011. Nitrogen flows from European regional watersheds to coastal marine waters. Chapter 13, European Nitrogen Assessment, Cambridge University Press.
- Blomqvist, S., A. Gunnars, and R. Elmgren. 2004. Why the limiting nutrient differs between temperate coastal seas and freshwater lakes: A matter of salt. *Limnol. Oceanogr.* **49**:2236–2241.
- Bowden, W.B. 1986. Gaseous nitrogen emissions from undisturbed terrestrial ecosystems: An assessment of their impacts on local and global nitrogen budgets. *Biogeochemistry* **2**:249-279
- Bowen, J.L. & I. Valiela. 2001. Historical changes in atmospheric nitrogen deposition to Cape Cod, Massachusetts, USA. *Atmospheric Environment* **35**: 1039-1051
- Boynton, W.R., J.H. Garber, R. Summers, and W.M. Kemp. 1995. Inputs, transformations and transport of nitrogen and phosphorus in Chesapeake Bay and selected tributaries. *Estuaries* **18(1B)**: 285-314
- Bricker, S.B., C.G. Clement, D.E. Pirhall, S.P. Orlando, and D.R.G Farrow. 1999. National estuarine eutrophication assessment: A summary of conditions, historical trends, and future outlook. Special Projects Office and National Centers for Coastal Ocean Sciences, National Ocean Service, National Oceanic and Atmospheric Administration.
- Bricker, S., B. Longstaff, W. Dennison, A. Jones, K. Boicourt, C. Wicks, and J. Woerner. 2007. Effects of Nutrient Enrichment In the Nation's Estuaries: A Decade of Change. NOAA Coastal Ocean Program Decision Analysis Series No. 26. National Centers for Coastal Ocean Science, Silver Spring, MD.
- Conley, D. J, H. W. Paerl, R. W. Howarth, D. F. Boesch, S. P. Seitzinger, K. E. Havens, C. Lancelot, and G. E. Likens. 2009. Controlling eutrophication: Nitrogen and phosphorus. *Science* **323**: 1014-1015.

Costello, C.T., and W.J. Kenworthy. 2011. Twelve-year mapping and change analysis of eelgrass (*Zostera marina*) areal abundance in Massachusetts (USA) identifies statewide declines. *Estuaries and Coasts* **34**: 232-242.

Cressie, N., and D.L. Zimmerman. 1992. On the Stability of the Geostatistical Method. *Mathematical Geology*. **24**: 45-59.

Currie, L.A. 1999. Nomenclature in evaluation of analytical methods including detection and quantification capabilities (IUPAC Recommendations 1995). *Analytica Chimica Acta* **391**: 105-126

Duarte, C. M. 1990. Seagrass nutrient content. *Marine Ecology Progress Series*. **67**: 201-207

Duarte C. M. 1995. Submerged aquatic vegetation in relation to different nutrient regimes. *Ophelia* **41**: 87-112.

Duarte, C. M., and J. Cebrián. 1996. The fate of marine autotrophic production. *Limnology and Oceanography*. **41**: 1758-1766.

Dudel, G. and J.G. Kohl. 1992. The nitrogen budget of a shallow lake (Grober Muggelsee, Berlin). *Int. Revue ges. Hydrobiol.* **77**: 43-72.

EPA Science Advisory Board. 2008. Hypoxia in the northern Gulf of Mexico: An update by the EPA Science Advisory Board. EPA-SAB-08-003. US Environmental Protection Agency, Science Advisory Board, Washington, DC.

Ganju, N.K. 2011. A novel approach for direct estimation of fresh groundwater discharge to an estuary. *Geophysical Research Letters*. **38**: L11402

Ganju, N.K, M. Hayn, S. Chen, R.W. Howarth, P.J. Dickhudt, C.R. Sherwood, A.L. Aretxabaleta, R. Marino. 2012. Tidal and groundwater fluxes to a shallow, microtidal estuary: constraining inputs through field observations and hydrodynamic modeling. *Estuaries and Coasts*. In press.

Gibb, S.W. and R.F.C. Mantoura. 1999. Ocean-atmosphere exchange and atmospheric speciation of ammonia and methylamines in the region of the NW Arabian Sea. *Global Biogeochemical Cycles* **13(1)**: 161-178

Gotvald, A.J. and K.A. Oberg. 2009. Acoustic Doppler Current Profiler Applications Used in Rivers and Estuaries by the U.S. Geological Survey: U.S. Geological Survey Fact Sheet, 2008-3096, 4 pp.

Hamilton R.P. 1995. Hydrodynamic and water quality study of West Falmouth Harbor, MA. Aubrey Consulting, Inc. Woods Hole, MA

Howarth, R.W., and R. Marino. 2006. Nitrogen as the limiting nutrient for eutrophication in coastal marine ecosystems: Evolving views over three decades. *Limnol. Oceanogr.* **51**: 364-376

Howarth, R.W., Chan, F., Conley, D.J., Garnier, J., Doney, S.C., Marino, R., and G. Billen. 2011. Coupled biogeochemical cycles: eutrophication and hypoxia in temperate estuaries and coastal marine ecosystems. *Frontiers in Ecology and the Environment.* **9(1)**:18-26

Howes B., S.W. Kelley, J.S. Ramsey, R. Samimy, D. Schlezinger, E. Eichner. 2006. Linked Watershed-Embayment Model to Determine Critical Nitrogen Loading Thresholds for West Falmouth Harbor, Falmouth, Massachusetts. Massachusetts Estuaries Project, Massachusetts Department of Environmental Protection. Boston, MA.

Jahne, B., K.O. Munnich, R. Bosinger, A. Dutzi, W. Huber, and P. Libner. 1987. On the parameters influencing air-water gas exchange. *Journal of Geophysical Research* **92**:1937-1949.

Jordan, M.J., K.J. Nadelhoffer, and B. Fry. 1997. Nitrogen cycling in forest and grass ecosystems irrigated with ¹⁵N-enriched wastewater. *Ecological Applications.* **7(3)**: 864-881

Kaluzny S.P., S.C. Vega, T.P. Cardoso, and A.A. Shelly. 1998. S+ Spatial Stats User's Manual for Windows and Unix. Springer, New York.

Koop-Jakobsen, K. 2003. Ammonium dynamics in tidal salt marshes – an experimental study of ammonium adsorption, tidal flushing, and ammonia volatilization. Masters Thesis. Roskilde University, Denmark.

Koroleff, F. 1983. Simultaneous oxidation of nitrogen and phosphorus compounds by persulfate. p.168-169. In K. Grasshoff, M. Eberhardt, and K. Kremling, eds., *Methods of Seawater Analysis*. 2nd ed., Verlag Chemie, Weinheimer, FRG.

Kroeger, K.D., M.L. Cole, and I. Valiela. 2006. Groundwater-transported dissolved organic nitrogen exports from coastal watersheds. *Limnology and Oceanography*. **51(5)**: 2248-2261

Kutner, M.H., C.J. Nachtsheim, and J. Neter. 2004. Applied Linear Regression Models. McGraw-Hill Irwin, Boston.

Larsen, R.K., J.C. Steinbacher, and J.E. Baker. 2001. Ammonia exchange between the atmosphere and the surface waters at two locations in the Chesapeake Bay. *Environmental Science and Technology* **35**: 4731-4738

Ledwell, J.J. 1984. The variation of the gas transfer coefficient with molecular diffusivity. In W. Brutsaert and G.H. Jirka (eds) Gas transfer at water surfaces. D. Reidel Publishing Co., Dordrecht.

Li, X., Z. Yu, X. Song, X. Cao, and Y. Yuan. 2011. Nitrogen and phosphorus budgets of the Changjiang River estuary. *Chinese Journal of Oceanology and Limnology*. **29(4)**: 762-774

Little L.S., D. Edwards, and D.E. Porter. 1997. Kriging in estuaries: as the crow flies, or as the fish swims? *Journal of Experimental Marine Biology and Ecology*, **213**: 1-11

Marino, R. and R.W. Howarth. 1993. Atmospheric oxygen exchange in the Hudson River: dome measurements and comparison with other natural waters. *Estuaries* **16(3A)**: 433-445

Marino, R. 2001. An experimental study of the role of phosphorus, molybdenum, and grazing as interacting controls on planktonic nitrogen fixation in estuaries. Ph. D. dissertation. Cornell University.

McGlathery KJ, Anderson IC, Tyler AC. 2001. Magnitude and variability of benthic and pelagic metabolism in a temperate coastal lagoon. *Marine Ecological Progress Series*. **216**: 1-15

McGlathery, K. J., K. Sundback, and I. C. Anderson. 2004. The importance of primary producers for benthic N and P cycling. In: The Influence of Primary Producers on Estuarine Nutrient Cycling, Nielsen, S.L., G.M. Banta, and M.F. Pedersen, (Eds.). Kluwer Academic Publishers.

McGlathery, K. J., K. Sundback, and I. C. Anderson. 2007. Eutrophication in shallow coastal bays and lagoons: the role of plants in the coastal filter. *Marine Ecological Progress Series*. **348**: 1-18.

McGlathery, K. J. 2008. Nitrogen cycling in seagrass meadows. In D. Capone, D. A. Bronk, M. R. Mulholland & E. J. Carpenter (eds.), *Nitrogen in the Marine Environment*, 2nd Edition, Elsevier, Oxford.

McGlathery, K.J., Berg, P. Giblin, A., Howarth, R.W., Marino, R., Foreman, K., and Hayn, M. 2009. Eutrophication effects on nitrogen assimilation and turnover in shallow coastal systems. Coastal and Estuarine Research Federation, Bi-Annual Conference. Portland, Oregon.

Murphy, M.A., and B.G. Brownlee. 1981. Ammonia volatilization in a hypertrophic prairie lake. *Canadian Journal of Fisheries and Aquatic Science*. **38**: 1035-1039

Nixon, S.W. 1995. Coastal marine eutrophication: A definition, social causes, and future concerns. *Ophelia*. **41**: 199-219.

Nixon, S. W., J. W. Ammerman, L. P. Atkinson, V. M. Berounsky, G. Billen, W. C. Boicourt, W. R. Boynton, T. M. Church, D. M. DiToro, R. Elmgren, J. H. Garber, A. E. Giblin, R. A. Jahnke, N. J. P. Owens, M. E. Q. Pilson, and S. P. Seitzinger. 1996. The fate of nitrogen and phosphorus at the land-sea margin of the North Atlantic Ocean. *Biogeochemistry*. **35**: 141-180.

Nixon, S.W., B. Buckley, S. Granger, and J. Bintz. 2001. Responses of very shallow marine ecosystems to nutrient enrichment. *Human and Ecological Risk Assessment*. **7**: 1457-1481.

NRC (National Research Council). 2000. *Clean Coastal Waters; understanding and reducing the effects of nutrient pollution*. Committee on the Causes and Management of Coastal Eutrophication. National Academy Press. Washington, D.C.

Paerl, H. W. 2009. Controlling eutrophication along the freshwater-marine continuum: dual nutrient (N and P) reductions are essential. *Estuaries and Coasts*. **32**: 593-601.

Pedersen, M.F., S.L. Nielsen, and G.T. Banta. 2004. Interactions between vegetation and nutrient dynamics in coastal marine ecosystems: an introduction. In: Nielsen SL, Banta GT, Pedersen MF (eds) *Estuarine nutrient cycling: the influence of primary producers*, Kluwer Academic, Dordrecht. p 1–16

Quinn, P.K., R.J. Charlson, and T.S. Bates. 1988. Simultaneous observations of ammonia in the atmosphere and ocean. *Nature*. 335:120-121.

- Rabalais, N.N. 2002. Nitrogen in aquatic ecosystems. *Ambio*. **31**: 102-112.
- Rathbun, S.L. 1998. Spatial Modeling in Irregularly Shaped Regions: Kriging Estuaries. *Environmetrics* **9**: 109-129
- Risgaard-Petersen N, Ottosen LDM (2000) Nitrogen cycling in two temperate *Zostera marina* beds: seasonal variation. *Marine Ecological Progress Series*. **198**: 93–107
- Ruhl, C.A., and M.R. Simpson. 2005. Computation of discharge using the index-velocity method in tidally affected areas: U.S. Geological Survey Scientific Investigations Report 2005-5004, 31p.
- Simpson, M.R. and R. Bland. 2000. Methods for accurate estimation of net discharge in a tidal channel. *IEEE Journal of Oceanic Engineering*. **25(4)**: 437-445
- Solorzano, L. 1969. Determination of ammonia in natural waters by the phenol hypochlorite method. *Limnology and Oceanography*. **14**: 799-801
- Stearns & Wheler, LLC Environmental Engineers and Scientists 2001. Town of Falmouth, MA. Wastewater Facilities Plan and Final Environmental Impact Report for Wastewater Facilities Planning Study. Unpublished report, 134 pp.
- Town of Falmouth. May 2011. Wastewater Department Website: 2. Current wastewater management in Falmouth. <http://www.falmouthmass.us/depart.php?depkey=wastewater>
- Valiela I., J. McClelland, J. Hauxwell, P.J. Behr, D. Hersh, and K. Foreman. 1997. Macroalgae blooms in shallow estuaries: Controls and ecophysiological and ecosystem consequences. *Limnology and Oceanography*. **42**: 1105–1118.
- Vitousek, P. M. & R. W. Howarth. 1991. Nitrogen limitation on land and in the sea. How can it occur? *Biogeochemistry*. **13**: 87-115.
- Watson, A.J., R.C. Upstill-Goddard, and P.S. Liss. 1991. Air-sea gas exchange in rough and stormy seas measured by a dual tracer technique. *Nature*. **349**:145-147.
- Weiskel, P.K. and B.L. Howes. 1992. Differential Transport of Sewage Derived Nitrogen and Phosphorous through a Coastal Watershed. *Environmental Science and Technology*. **26(2)**: 352 – 360.

Zhuang, L., and B.J. Huebert. 1996. Lagrangian analysis of the total ammonia budget during Atlantic Stratocumulus Transition Experiment / Marine Aerosol and Gas Exchange. *Journal of Geophysical Research*. **101**: 4341-4350